



Title	Chiral anomaly-induced magnetotransport in Dirac and Weyl semimetals
Author(s)	鍵村, 亜矢
Citation	大阪大学, 2018, 博士論文
Version Type	VoR
URL	<a href="https://doi.org/10.18910/69326">https://doi.org/10.18910/69326</a>
rights	
Note	

*The University of Osaka Institutional Knowledge Archive : OUKA*

<https://ir.library.osaka-u.ac.jp/>

The University of Osaka

Ph. D. Thesis

Chiral anomaly-induced magnetotransport in  
Dirac and Weyl semimetals

Aya Kagimura<sup>1</sup>

Osaka University Particle Physics Theory Group

February 27, 2018

---

<sup>1</sup>kagimura@het.phys.sci.osaka-u.ac.jp

## Abstract

In 1983, Nielsen and Ninomiya pointed out that there is the effect coming from the same mechanism as the chiral anomaly in condensed matter systems [1]. They predicted that the external magnetic field generate the electric current proportional to the chiral anomaly in band structure which possesses two Weyl nodes with the opposite chiralities when there is difference of the Fermi energy between the left-handed fermion and the right-handed fermion. Nowadays this phenomenon called chiral magnetic effect attracts a lot of interest, which emerges not only in condensed matter systems but also in other systems which possesses the chiral fermion such as quark-gluon plasma and the early universe. The series of discoveries of the Dirac or Weyl semimetals begun from 2013 enable us to observe the chiral magnetic effect in the condensed matter experiments. The Dirac or Weyl semimetals possess the massless Dirac or Weyl fermions as low energy excitations. In such relativistic fermion systems, the transport phenomenon under the external magnetic field shows peculiar behavior as Nielsen and Ninomiya pointed out. To estimate the conductivity due to the chiral magnetic effect, it is necessary to calculate the relaxation in the magnetic field. The relaxation time calculated in 1950s by Argyres and Adams [2] are insufficient to estimate the chiral magnetic effect which emerges in the relativistic fermion system, because it is calculated only for the non-relativistic fermion in ultra-quantum limit. To estimate the chiral magnetic effect in the Weyl semimetals, the calculation is highly dependent on the materials and its modeling, because only inter-cone transition contribute to the relaxation. Recently many papers provided the relativistic calculation of the relaxation time in the magnetic field using the models of the Weyl semimetals.

In this thesis, we investigate the chiral anomaly-induced electric charge transport phenomenon along the external magnetic field in Dirac semimetals [3]. Extending the work by Argyres and Adams, we provide the model-independent calculation of the relaxation time away from the strong magnetic field limit in the relativistic low energy effective theory. In strong magnetic field limit, intra-cone transition does not occur for the exact massless fermion because of the helicity conservation. In that case, the transport phenomenon is affected by the inter-cone transition which is depend on the lattice structure. For model-independent prediction, we investigate the transport of the fermion with a small mass realized in the slightly distorted Dirac semimetals in the presence of Coulomb impurities. Using the semi-classical Boltzmann equation, we derive the relaxation time for two kinds of intra-cone transition. One is due to the effect of mass, and the other is due to the excited states of Landau levels away from the strong magnetic field limit. Deriving the analytic formula for the intra-cone transition, we find that the small mass causes the helicity flipping by the intra-cone transition. We also find that the intra-cone transition through the excited states in Landau levels works as a mechanism of the helicity flipping away from the strong magnetic field limit, which remains finite in the massless limit. We derive the mass and the magnetic field dependence of the longitudinal magnetoconductivity in the presence of the parallel electric field and magnetic field.

# Contents

<b>1</b>	<b>Introduction</b>	<b>3</b>
<b>I</b>	<b>Review on Chiral Anomaly and Massless Fermions in Solid</b>	<b>7</b>
<b>2</b>	<b>Dirac Semimetal and Weyl Semimetal</b>	<b>7</b>
2.1	Energy band of the Dirac and Weyl semimetals . . . . .	7
2.2	Effective Hamiltonian for Weyl fermions . . . . .	8
2.3	Kramers degeneracy . . . . .	12
2.4	Symmetry protected Dirac semimetals . . . . .	14
<b>3</b>	<b>Magnetotransport Induced by Chiral Anomaly</b>	<b>17</b>
3.1	Macroscopic explanation of the chiral anomaly . . . . .	18
3.2	Electric current induced by chiral anomaly . . . . .	21
3.3	Previous study for relaxation time . . . . .	24
<b>II</b>	<b>Calculation of Relaxation Time</b>	<b>27</b>
<b>4</b>	<b>Massive Dirac Fermion and Transport Theory</b>	<b>27</b>
4.1	Massive Dirac fermion in the magnetic field . . . . .	28
4.2	Basics of the transport theory . . . . .	30
<b>5</b>	<b>Relaxation time for massive fermion in strong magnetic field</b>	<b>33</b>
<b>6</b>	<b>Magnetoconductivity in Weaker Magnetic Field</b>	<b>37</b>
<b>7</b>	<b>Summary and Discussion</b>	<b>43</b>
<b>A</b>	<b>Formulae for <math>I(\gamma)</math></b>	<b>46</b>
<b>B</b>	<b>Solution of Equations for Relaxation Times</b>	<b>47</b>

# 1 Introduction

Chiral anomaly or Adler-Bell-Jackiw anomaly [4, 5], which was discovered in 1969, is an important concept in gauge theories. The physical consequence of the chiral anomaly is that for massless fermions coupled with the electromagnetic gauge field, the chiral fermion number  $N_5$  is not conserved but obeys the anomaly equation

$$\frac{dN_5}{dt} = \frac{e^2}{2\pi^2} \mathbf{E} \cdot \mathbf{B}. \quad (1.1)$$

In 1983 Nielsen and Ninomiya pointed out that condensed matter systems have an effect which arises essentially from the same mechanism of the chiral anomaly [1]. They considered a band structure with two Weyl nodes which possess the opposite chirality, applying the parallel electric and magnetic field. The fermion states are quantized by the magnetic field to form Landau levels, and the fermion gets drifted by the electric field within a given level. Then the equation for chiral fermion number completely matches with Eq.(1.1). At the same time, drifted fermions get scattered back by impurities, acoustic phonons, or other electrons. The balance between the drift and the scattering determines the magnitude of the electric current measured in observation. They predicted the enhancement of the magnetoconductivity proportional to  $\mathbf{E} \cdot \mathbf{B}$  caused by the chiral anomaly effect.

Their prediction had not been tested in the observation for 30 years, because the example of Weyl nodes had not been discovered in solids. The recent study of the topological band structure and the Berry curvature changed the situation. The topology is a property preserved under the continuous deformation, which appears in the context of the physics, and provides the strong constraint to many physical systems. For example, the quantum anomaly including the chiral anomaly is one of the example of the consequence coming from the topology of the gauge field configuration. In condensed matter system, it was clarified that the quantum Hall effect arises essentially from the fact that the wave function describing the two dimensional electronic system under the magnetic field has the non-trivial topology [6]. Recently, consideration of the topology has yielded the discovery of the interesting material which is insulating in the bulk and has the two dimensional gapless excitation in the surface [7, 8]. Such topological insulator occurs in the presence of the strong spin orbit interaction in certain materials with the unbroken time reversal symmetry.

The interest of Weyl semimetals has begun with theoretical proposal by Wan et al. [9] in 2011. The Weyl semimetal which is a new kind of the topological matter possess a pair of three dimensional massless excitations with the opposite chirality at separated point in the momentum space. From the similarity of the appearance of a pair of the gapless two component excitation, the Weyl semimetals are mentioned as the three dimensional graphene [10, 11]. Based on the first-principles calculation they have proposed  $\text{Y}_2\text{Ir}_2\text{O}_7$  where the experiments indicate the magnetic order [12] which breaks the time reversal symmetry, as a candidate of the Weyl semimetal. Their proposal has led to the study of various materials for the realization of the Weyl semimetals both in theory [13, 14, 15, 16, 17, 18] and experiments [19, 20, 21, 22, 23, 24].

On the other hand, the realization of the Dirac semimetal which possess a three dimensional massless Dirac node composed of a pair of Weyl nodes at the same point in the momentum space was proposed by the careful studies of the topological phase transition between a three dimensional topological insulator and a normal insulator with both the time

reversal and spatial inversion symmetry [25, 26, 27]. It is demonstrated that the three dimensional Dirac semimetal is realized at a critical point where the phase transition occurs, requiring the very detailed fine tuning of the chemical compositions [28, 29]. From the theoretical studies, it was also found the three dimensional gapless Dirac node [30, 31] protected by the crystalline symmetry. The detailed symmetry analysis of  $\text{Na}_3\text{Bi}$  [32] and  $\text{Cd}_3\text{As}_2$  [33] by Wang et al. has shown that it has the stable three dimensional Dirac nodes. These predictions have led to the discovery of the stable three dimensional Dirac semimetals in  $\text{Na}_3\text{Bi}$  [34, 35] and  $\text{Cd}_3\text{As}_2$  [36, 37, 38, 39, 40] in the experiments. Since these Dirac semimetals are protected by the crystalline symmetry, it is theoretically predicted that the breaking of rotational crystalline symmetry by the mechanical strain open a gap at the Dirac point [32, 40, 41, 42].

The chiral anomaly-induced negative magnetoresistance was firstly observed in  $\text{Bi}_{0.97}\text{Sb}_{0.03}$  crystal [43] which is the unstable Dirac semimetal without the protection by the rotational crystalline symmetry. They reported the increase of the conductivity induced by the chiral anomaly in the strong magnetic field region ( $B > 0.4T$ ) when the magnetic field is applied parallel to the electric field. In addition, the maximum of the conductivity in the weak magnetic field region ( $B < 0.4T$ ) is also detected. Similar feature of the unusual magnetoresistance is observed in another unstable Dirac semimetal  $\text{ZrTe}_5$  [44], the stable Dirac semimetals  $\text{Na}_3\text{Bi}$  [45] and  $\text{Cd}_3\text{As}_2$  [46], and in the Weyl semimetals, such as  $\text{TaAs}$  [47, 48],  $\text{TaP}$  [49],  $\text{NbAs}$  [50, 51],  $\text{NbP}$  [50] and  $\text{WTe}_2$  [52, 53].

The transport property plays an important role in helping us to understand the application possibilities of the Weyl or Dirac semimetals. The Weyl or Dirac semimetals have symmetry protected topological phase, and since their transport phenomena is robust against the perturbation of the environment, they are expected to be applied to the ideally low cost device. Therefore it is important to compare the characteristics of the magnetotransport in the experimental observations to theoretical predictions. The observed negative magnetoconductivity in the weak magnetic field region is not perfectly understood. For the Weyl semimetals it is explained as the result of the weak anti-localization effect [54] in zero magnetic field, which is the mechanism to suppress the back scattering. The mechanism of the weak anti-localization effect is as following. The interference term between the process from the state with momentum  $\mathbf{k}$  to the state with momentum  $-\mathbf{k}$  through the multiple scattering and its time reversed process get the Berry phase  $\pm\pi$  for the Weyl node with the monopole charge  $\pm 1$ . Due to the Berry phase, the quantum correction to the probability of the back scattering get a minus sign, which is named weak anti-localization effect [55]. Therefore, since this effect disappears under the magnetic field which breaks the time reversal symmetry, the magnetoconductivity becomes negative.

On the other hand, since the Dirac semimetal has the degenerated states at all momentum  $\mathbf{k}$ , it has two states with the momentum  $-\mathbf{k}$ ; one is the time reversed state and the other is not connected with the original state by the time reversal symmetry. When one consider the back scattering to the non-time reversal state, since it does not get the Berry phase, the correction to the probability of this back scattering becomes positive. Therefore the correction to the conductivity in zero magnetic field from the two back scattering is completely cancelled each other [56]. So the Dirac and Weyl semimetals could have different mechanisms of the negative magnetoconductivity in the weak magnetic field region.

To make a theoretical prediction at the quantitative level, one needs to know the relaxation time. It is a rather difficult problem, since the relaxation occurs through transition

between Weyl (or Dirac) cones at different momentum points in the Brillouin zone (called as ‘inter-cone transition’), which is highly dependent on the material as well as its modeling. There are several papers calculating the scattering amplitude of the fermion in the magnetic field [2, 57, 58, 59, 60, 61] under various conditions, where most of these calculations are based on certain models of the Weyl semimetal. It would be nice if we can predict some universal feature of the magnetoconductivity which is model independent. Although an early calculation in 1956 [2] is the general calculation using the effective theory, it is unsatisfactory since it was estimated for non-relativistic fermions in the ultra-quantum limit where only the lowest Landau state contribute to the scattering. Since the experiment measures the magnetoconductivity of semimetals for a wide range of the magnetic field strength, it is needed to predict the relaxation time for electrons in the Dirac or Weyl semimetals with the magnetic field both in and away from the quantum limit.

To observe the anomaly-induced negative magnetoresistance it is necessary that the sufficiently low Fermi energy is given into the system. In fact even in the same material  $\text{Cd}_3\text{As}_2$ , when its carrier density is very high, the behavior of the observed longitudinal magnetoresistance is not negative, but the usual Shubnikov de Haas oscillation [62]. This experiment indicates that when the lowest Landau level is hidden under the Fermi energy, the negative magnetoresistance due to the chiral anomaly does not emerge. This is consistent with Nielsen and Ninomiya’s discussion which considers only the lowest Landau state. We would like to address the middle range between the case with the very high Fermi energy and the case in the ultra-quantum limit to investigate the start of the chiral magnetic effect.

Besides, since the realization of the unstable Dirac semimetals requires the very detailed fine tuning of the parameter, the Dirac semimetals used in the experiments [43, 44] have the possibility of the small gap opening. Even in the stable Dirac semimetals, the magnetic field should be applied along a certain direction which preserve the crystalline symmetry which protect the gapless Dirac nodes. Since when the magnetic field direction is deviated from the symmetric direction, the Dirac semimetals used in the experiments [32, 33] may have very small mass gap. Therefore we would also like to estimate the effect of the mass gap of the Dirac fermion to the magnetoconductivity.

For this purpose, we focus on the effects on the magnetoconductivity for the Dirac semimetals due to the change of external parameters such as the magnetic field or mass gap by breaking the crystalline rotational symmetry [32, 40, 41, 63, 42]. We can expect that the change from the ideal magnetoresistance is triggered by the onset of ‘intra-cone transition’ so that the effects can be described by the low energy effective theory for the single Dirac cone. Using the action for relativistic Dirac fermion as the low energy effective theory, we derive a general formula for the relaxation time due to impurities for the Dirac semimetal with mass gap  $m$  from mechanical strain and under magnetic field  $B$  including the regime away from the quantum limit. Using our formula, we predict a drastic change in the magnetoconductivity. Although there has yet been no clear experimental observation of such effects, our prediction may offer a deeper understanding of the magnetoconductivity as well as interesting technological applications.

In theoretical development, the chiral anomaly contribution to conductivity is discussed in chiral kinetic theory [64, 65, 66]. This phenomena is now called chiral magnetic effect and is now getting a renewed interest in the quark gluon plasma [67, 68, 69], the electroweak plasma in early universe [70], and neutrinos in supernovae [71]. Besides, the negative magnetoresistance in multilayer Dirac electron systems considered in Ref. [72]. The chiral

magnetic effect in the Weyl or Dirac semimetals is an interesting topic not only as the demonstration of the chiral anomaly in the low energy experiment, but also as potential applications in “valleytronic” devices [73]. Our approach may also be extended to these systems.

This thesis is organized as follows. In Sec.2, starting from the general Hamiltonian for the topological insulator, we review the realization of the effective Hamiltonian for the Dirac and Weyl semimetals. In sec.3, reviewing the basics of the transport theory, we explain how it is related to chiral anomaly as discussed in Ref. [1]. In part II, we give details of our calculation and the results of the relaxation time following the published paper [3]. In Sec.4, we derive the relation between the electric current and the relaxation times when multiple Landau levels cross the Fermi energy. In Sec.5, we give details of the calculation of the scattering amplitude and relaxation time for a relativistic fermion with a small mass in strong magnetic field region. The magnetic field dependence of the magnetoconductivity in weak magnetic field are shown in Sec.6. Finally, we summarize our study and give a discussion in Sec.7.

## Part I

# Review on Chiral Anomaly and Massless Fermions in Solid

## 2 Dirac Semimetal and Weyl Semimetal

In this section, we review that a magnetic impurity doped topological insulator has a energy dispersion relation of Weyl semimetal which is characterized by pairs of gapless nodes. We also see that the degeneracy of the Dirac semimetal is a consequence of the time reversal and parity symmetry of the system and that further crystalline symmetry is required for the stable Dirac semimetals.

### 2.1 Energy band of the Dirac and Weyl semimetals

We will see that the effective Hamiltonian for the topological insulator and the spin splitting term induced by the magnetic impurity leads to an energy dispersion relation of the Weyl semimetal. In this subsection, we follow the discussion in Ref.[74].

The effective Hamiltonian describing the electron states in topological insulator is generally written by the following form

$$\mathcal{H}_{\text{TI}} = R_\mu(\mathbf{k})\alpha_\mu, \quad (2.1)$$

where

$$\begin{aligned} \alpha_i &= -\tau_3 \otimes \sigma_i = \begin{pmatrix} -\sigma_i & 0 \\ 0 & \sigma_i \end{pmatrix}, \text{ for } i = 1, 2, 3, \\ \alpha_0 &= \tau_1 \otimes \sigma_0 = \begin{pmatrix} 0 & 1 \\ 1 & 0 \end{pmatrix}, \end{aligned}$$

where  $\tau_i, \sigma_i$  are the Pauli matrices and  $\tau_0, \sigma_0$  are  $2 \times 2$  identity matrices.  $\tau_i$  and  $\sigma_i$  represent the orbital and spin degrees of freedom, respectively. When the magnetic impurities are doped, the spin splitting term

$$b\Sigma_3 = b\tau_0 \otimes \sigma_3 = b \begin{pmatrix} \sigma_3 & 0 \\ 0 & \sigma_3 \end{pmatrix}, \quad (2.2)$$

arises. We derive the energy eigenvalue of the total Hamiltonian  $\mathcal{H}_{\text{TI}} + b\Sigma_3$ . Using the properties of  $\alpha_\mu$  and  $\sigma_3$ , we find

$$\mathcal{H}^2 = R_\mu R_\mu + b^2 + b(R_3\{\alpha_3, \Sigma_3\} + R_0\{\alpha_0, \Sigma_3\}). \quad (2.3)$$

Notice that the eigenvalue of  $R_3\{\alpha_3, \Sigma_3\} + R_0\{\alpha_0, \Sigma_3\}$  is  $\pm 2\sqrt{R_3^2 + R_0^2}$ , because

$$(R_3\{\alpha_3, \Sigma_3\} + R_0\{\alpha_0, \Sigma_3\})^2 = 4(R_3^2 + R_0^2).$$

Then we obtain the energy eigenvalue

$$\epsilon^2 = R_1^2 + R_2^2 + \left( b \pm \sqrt{R_3^2 + R_0^2} \right)^2. \quad (2.4)$$

Then the Weyl points are determined by the condition

$$R_1 = R_2 = \sqrt{R_3^2 + R_0^2} - |b| = 0. \quad (2.5)$$

Let us take

$$R_i = \frac{1}{a} \sin ak_i, \quad R_0 = \frac{M}{a} + \frac{r}{a} \sum_{i=1}^3 (1 - \cos ak_i), \quad (2.6)$$

where  $a$  is a lattice constant. In continuum limit,  $R_i \rightarrow k_i$ ,  $R_0 \rightarrow M$ , the energy goes to

$$\epsilon^2 = k_1^2 + k_2^2 + \left( \sqrt{k_3^2 + M^2} \pm b \right)^2. \quad (2.7)$$

We find that when  $|b|$  is larger than  $|M|$ , the gap close[Fig:1] at two points

$$\mathbf{k} = (0, 0, \pm\sqrt{b^2 - M^2}),$$

and so the Hamiltonian describes the Weyl semimetal. When  $|b|$  is smaller than  $|M|$ , the gap never close at any points in momentum space[Fig:2] and it is the case for the insulator. When both  $b$  and  $M$  is zero, the energy band is doubly degenerate at any points in momentum space and the gap close[Fig:3] at a point

$$\mathbf{k} = (0, 0, 0).$$

This is the energy band for the Dirac semimetal. However since the gapless state requires very detailed fine tuning of the parameters  $b$  and  $M$ , the Dirac node is unstable and a band gap opens in general. Therefore, an additional crystalline symmetry is required to realize the stable Dirac semimetal.

## 2.2 Effective Hamiltonian for Weyl fermions

We consider the case where the Fermi energy is zero, which is a natural situation without any doping. In this subsection, we derive the effective Hamiltonian for around the Weyl nodes at

$$\mathbf{K}_0 = (0, 0, \sqrt{b^2 - M^2}).$$

We obtain the energy eigenvalues  $\epsilon_i(\mathbf{k})$  which satisfy

$$(\mathcal{H}_{TI} + b\Sigma_3)|u_i(\mathbf{k})\rangle = \epsilon_i(\mathbf{k})|u_i(\mathbf{k})\rangle,$$

where  $|u_i(\mathbf{k})\rangle$ s are the energy eigenstate. There are four bands and two of these are degenerated on the Weyl nodes  $\pm\mathbf{K}_0$ ,

$$\epsilon_1(\pm\mathbf{K}_0) = 2|b|, \quad \epsilon_2(\pm\mathbf{K}_0) = \epsilon_3(\pm\mathbf{K}_0) = 0, \quad \epsilon_4(\pm\mathbf{K}_0) = -2|b|.$$

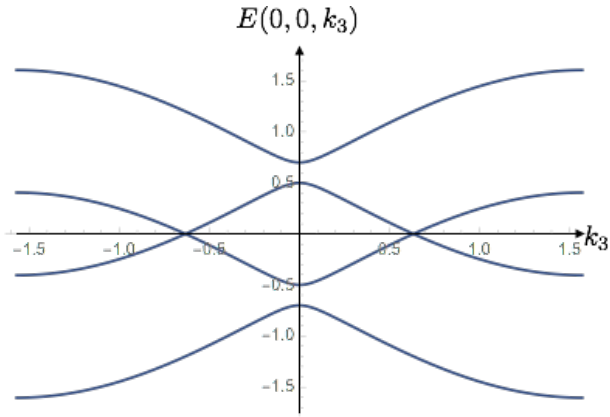


Figure 1: The energy band for the Weyl semimetal.

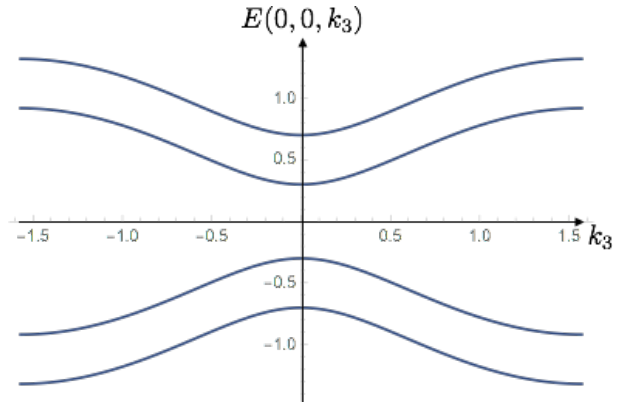


Figure 2: The energy band for the insulator.

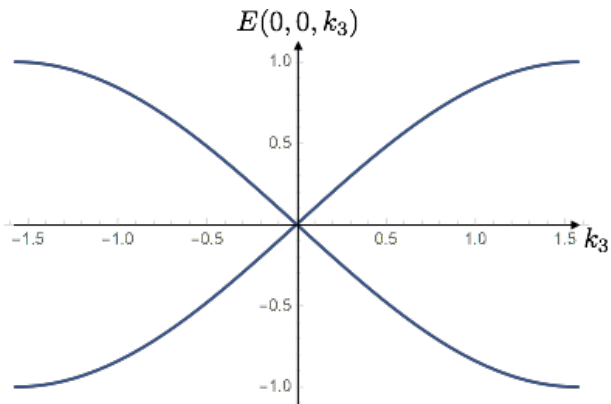


Figure 3: The energy band for the Dirac semimetal. It is doubly degenerate in any  $k_z$ .

Since only the states with the energy near the Fermi level affect the low energy physics, the states  $|u_1(\mathbf{k})\rangle$ ,  $|u_4(\mathbf{k})\rangle$  can be ignored in order to find the low energy effective Hamiltonian. Then around  $\mathbf{k} \sim \pm \mathbf{K}_0$ , the Hamiltonian can be reduced to two level Hamiltonian with the eigenvalues  $\epsilon_2(\mathbf{k})$ ,  $\epsilon_3(\mathbf{k})$ .

We first consider the effective Hamiltonian around  $\mathbf{k} \sim +\mathbf{K}_0$ . When  $k_1 = k_2 = 0$ , the energy is

$$\begin{aligned}\epsilon_2(k_1 = 0, k_2 = 0, k_3) &= \sqrt{k_3^2 + M^2} - |b| \approx \frac{\sqrt{b^2 - M^2}}{|b|} (k_3 - \sqrt{b^2 - M^2}), \\ \epsilon_3(k_1 = 0, k_2 = 0, k_3) &= -\left(\sqrt{k_3^2 + M^2} - |b|\right) \approx -\frac{\sqrt{b^2 - M^2}}{|b|} (k_3 - \sqrt{b^2 - M^2}),\end{aligned}$$

around  $k_3 \sim \sqrt{b^2 - M^2}$ . Therefore, defining the effective momentum

$$\mathbf{p} = \left( k_1, k_2, \frac{\sqrt{b^2 - M^2}}{|b|} (k_3 - \sqrt{b^2 - M^2}) \right),$$

we find the right-handed Weyl Hamiltonian

$$\mathcal{H}_R^{\text{Weyl}} = \mathbf{p} \cdot \boldsymbol{\sigma}. \quad (2.8)$$

Similarly around  $\mathbf{k} \sim -\mathbf{K}_0$ , since

$$\begin{aligned}\epsilon_2(k_1 = 0, k_2 = 0, k_3) &\approx -\frac{\sqrt{b^2 - M^2}}{|b|} (k_3 + \sqrt{b^2 - M^2}), \\ \epsilon_3(k_1 = 0, k_2 = 0, k_3) &\approx \frac{\sqrt{b^2 - M^2}}{|b|} (k_3 + \sqrt{b^2 - M^2}),\end{aligned}$$

at  $k_1 = k_2 = 0$ , we define the effective momentum

$$\mathbf{p} = -\left( k_1, k_2, -\frac{\sqrt{b^2 - M^2}}{|b|} (k_3 + \sqrt{b^2 - M^2}) \right),$$

where the overall  $-$  sign is set in order to keep the right-handed coordinate system. Then the effective Hamiltonian is obtained as the left-handed Weyl Hamiltonian

$$\mathcal{H}_L^{\text{Weyl}} = -\mathbf{p} \cdot \boldsymbol{\sigma}. \quad (2.9)$$

Finally we obtain two Weyl fermions with the chirality  $\pm 1$  at the points  $\pm \mathbf{K}_0$ , respectively. We notice that even when the mass term  $m\sigma_3$  is added, the Weyl nodes merely shift within  $z$  axis and the mass gap does not open. Therefore the existence of the Weyl points and gapless linear dispersion is robust against the perturbations in contrast to the Dirac semimetals.

The eigenfunctions of the right-handed Weyl Hamiltonian (2.8) are given by

$$|+, \mathbf{p}\rangle = e^{-i\psi/2} \begin{pmatrix} e^{-i\phi/2} \cos \frac{\theta}{2} \\ e^{+i\phi/2} \sin \frac{\theta}{2} \end{pmatrix}, \quad |-, \mathbf{p}\rangle = e^{-i\psi/2} \begin{pmatrix} e^{-i\phi/2} \sin \frac{\theta}{2} \\ e^{+i\phi/2} \cos \frac{\theta}{2} \end{pmatrix},$$

where we use the polar coordinate in momentum space and overall phase factor  $e^{-i\psi/2}$  is the gauge degrees of freedom. We consider the Berry connection for the valence band  $|\mathbf{p}, -\rangle$  which is occupied by the fermions

$$\begin{aligned}\mathbf{A}_-(\mathbf{p}) &:= -i\langle \mathbf{p}, - | \nabla_p | \mathbf{p}, - \rangle \\ &= -i \sin \frac{\theta}{2} \left( -i \sin \frac{\theta}{2} \nabla_p \frac{\psi}{2} - i \sin \frac{\theta}{2} \nabla_p \frac{\phi}{2} + \cos \frac{\theta}{2} \nabla_p \frac{\theta}{2} \right) \\ &\quad -i \cos \frac{\theta}{2} \left( -i \cos \frac{\theta}{2} \nabla_p \frac{\psi}{2} + i \cos \frac{\theta}{2} \nabla_p \frac{\phi}{2} - \sin \frac{\theta}{2} \nabla_p \frac{\theta}{2} \right) \\ &= -\frac{1}{2} (\nabla_p \psi - \cos \theta \nabla_p \phi).\end{aligned}$$

If we take the gauge as

$$\psi = \phi,$$

then we find the Berry connection

$$\mathbf{A}_-^N(\mathbf{p}) = -\frac{1}{2}(1 - \cos \theta) \nabla_p \phi = -\frac{1 - \cos \theta}{2p \sin \theta} \mathbf{e}_\phi,$$

where the  $\mathbf{e}_\phi$  is the unit vector in  $\phi$  direction. Since this is singular at the south pole

$$\theta = \pi,$$

we can use it for the northern hemisphere. For the southern hemisphere, taking the gauge

$$\psi = -\phi,$$

we can define the Berry connection

$$\mathbf{A}_-^S(\mathbf{p}) = \frac{1}{2}(1 + \cos \theta) \nabla_p \phi = \frac{1 + \cos \theta}{2p \sin \theta} \mathbf{e}_\phi,$$

where this is singular at the north pole

$$\theta = 0.$$

The Berry curvature is defined both in northern and southern hemisphere as

$$\begin{aligned}\mathbf{B}_R(\mathbf{p}) &= \nabla_p \times \mathbf{A}_-^N = \nabla_p \times \mathbf{A}_-^S \\ &= -\frac{1}{2} \frac{\mathbf{p}}{p^3}.\end{aligned}$$

For the eigenstates of the left-handed Weyl Hamiltonian (2.9), we obtain the Berry curvature by flipping the sign of the momentum  $\mathbf{p}$

$$\mathbf{B}_L(\mathbf{p}) = \frac{1}{2} \frac{\mathbf{p}}{p^3}.$$

Therefore we can define a ‘monopole’ in momentum space as

$$\rho_M^{R/L}(\mathbf{p}) = \frac{1}{2\pi} \nabla \cdot \mathbf{B}(\mathbf{p}) = \mp \delta(\mathbf{p}).$$

Integrating it over  $V$  which contains the Weyl nodes

$$\begin{aligned} \lambda &= -\frac{1}{2\pi} \int_V dV \nabla \cdot \mathbf{B} \\ &= -\frac{1}{2\pi} \int_{\partial V} d\mathbf{S} \cdot \mathbf{B} = \pm 1 \end{aligned}$$

gives the chirality of the occupied states around the Weyl nodes. Namely, the Weyl nodes in the momentum space is characterized by the monopole and anti-monopole in terms of the Berry curvature.

### 2.3 Kramers degeneracy

In this subsection, we show that the degeneracy for all momentum in the Dirac semimetal is a consequence of the time reversal and parity symmetry.

Define the time reversal transformation as  $\mathbf{x} \rightarrow \mathbf{x}$ ,  $\mathbf{p} \rightarrow -\mathbf{p}$ ,  $\boldsymbol{\sigma} \rightarrow -\boldsymbol{\sigma}$ , where  $\mathbf{x}$ ,  $\mathbf{p}$ ,  $\boldsymbol{\sigma}$  are the position, momentum, spin operator, respectively. If we consider a scalar, we can define the time reversal operator  $T$  as the complex conjugate operator  $K$ :

$$KiK^{-1} = -i.$$

Then since the momentum operator  $\mathbf{p}$  is given by  $-i\partial/\partial\mathbf{x}$  in the position space representation, we obtain the transformation

$$\mathbf{x} \rightarrow \mathbf{x}, \quad \mathbf{p} \rightarrow -\mathbf{p}.$$

On the other hand, in the case that we consider the fermion with the spin 1/2, since the spin operator is given by the Pauli matrices  $\sigma_i$ , complex conjugate operator flips the sign of the spin only in  $y$  direction. Therefore, defining

$$T = -i\sigma_2 K,$$

and then

$$T^{-1} = i\sigma_2 K,$$

we obtain the complete time reversal transformation we asked for:

$$\begin{aligned} T\mathbf{x}T^{-1} &= \mathbf{x}, \\ T\mathbf{p}T^{-1} &= -\mathbf{p}, \\ T\boldsymbol{\sigma}T^{-1} &= -\boldsymbol{\sigma}. \end{aligned} \tag{2.10}$$

We notice that the time reversal operator for spin 1/2 particle satisfy

$$T^2 = -1. \tag{2.11}$$

We consider the case that the system has the time reversal symmetry, which means the Hamiltonian commutes with the time reversal operator. When the time reversal operator acts on an eigenstate of the Hamiltonian  $|n\rangle$  with the energy eigenvalue  $\epsilon_n$ , the time reversed state  $T|n\rangle$  is also an eigenstate of the Hamiltonian  $H$  with the same energy eigenvalue  $\epsilon_n$ , because

$$HT|n\rangle = TH|n\rangle = \epsilon T|n\rangle.$$

If the time reversed state is the same state with the original state  $|n\rangle$ , it can be written by

$$T|n\rangle = e^{i\theta}|n\rangle.$$

When the time reversal operator acts on it again,

$$TT|n\rangle = T(e^{i\theta}|n\rangle) = e^{-i\theta}T|n\rangle = e^{-i\theta}e^{i\theta}|n\rangle = |n\rangle.$$

This is inconsistent with Eq.(2.11). Therefore we find the time reversed state is a different state with the original state, which means that when the system has the time reversal symmetry the energy eigenstate must be at least doubly degenerated. This degeneracy due to the time reversal symmetry is known as Kramers degeneracy.

We also define parity transformation  $\mathbf{x} \rightarrow -\mathbf{x}$ ,  $\mathbf{p} \rightarrow -\mathbf{p}$ ,  $\boldsymbol{\sigma} \rightarrow \boldsymbol{\sigma}$ . When the parity transformation operator  $P$  acts on an energy eigenstate, the transformed state is also the energy eigenstate in the system with parity symmetry. When the parity transformation and time reversal operator act on the energy eigenstate, since its momentum is flipped twice, the momentum of transformed state is the same as one of the original state. We know the transformed state is different state from original state by the discussion of the Kramers degeneracy. Therefore we find in the system with both parity and time reversal symmetry, the energy band is doubly degenerated for all momentum.

Let us consider the Hamiltonian  $\mathcal{H}_{\text{TI}} + b\Sigma_3$  introduced in the previous subsection. When the parity transformation operator in this representation can be written by

$$P = \begin{pmatrix} 1 & 0 \\ 0 & -1 \end{pmatrix}, \quad (2.12)$$

$\alpha_{1,2,3}$  anticommute with the parity transformation operator, and  $\alpha_0$  and  $\Sigma_3$  commute with it. When  $R_\mu(\mathbf{k})$  is given by Eq.(2.6), we find

$$R_{1,2,3}(-\mathbf{k}) = -R_{1,2,3}(\mathbf{k}), \quad R_4(-\mathbf{k}) = R_0(\mathbf{k}). \quad (2.13)$$

Therefore the Hamiltonian  $\mathcal{H}_{\text{TI}} + b\Sigma_3$  commutes with the parity transformation operator:

$$P(\mathcal{H}_{\text{TI}}(-\mathbf{k}) + b\Sigma_3)P^{-1} = \mathcal{H}_{\text{TI}}(\mathbf{k}) + b\Sigma_3, \quad (2.14)$$

which means that the system of the Weyl semimetal has the parity symmetry. On the other hand, since the time reversal operator for  $4 \times 4$  matrices can be written by

$$T = -i\tau_0 \otimes \sigma_2 K = \begin{pmatrix} -i\sigma_2 & 0 \\ 0 & -i\sigma_2 \end{pmatrix} K, \quad (2.15)$$

we find that it commutes with  $\alpha_{1,2,3}$  and anti-commutes with  $\alpha_0$  and  $\Sigma_3$ . Therefore without spin splitting term  $b\Sigma_3$  the Hamiltonian  $\mathcal{H}_{\text{TI}}$  commutes with the time reversal operator, and

the system has time reversal symmetry. As a consequence of the Kramers degeneracy and parity symmetry, the band structure of the Dirac semimetal is completely degenerated for all momentum. However the spin splitting term  $b\Sigma_3$  breaks the time reversal symmetry, and then the band structure of the Weyl semimetal has isolated degenerate points not for all momentum.

We notice that the parity and time reversal symmetry are not enough to protect the Dirac point. Since  $\alpha_0$  commutes with time reversal and parity transformation operators, the mass term cannot be prohibited by these symmetries. Further crystalline symmetry is necessary for the stable Dirac semimetals[30, 32, 33], and when the mechanical strain breaking the symmetry is applied a gap can open up[63].

## 2.4 Symmetry protected Dirac semimetals

In this subsection, we will see more general principles to create the three dimensional Dirac semimetals in the system with both the time reversal and the parity symmetry. Following the classification procedure of the stable three dimensional Dirac semimetals in Ref.[75], we will see how to obtain a stable Dirac semimetal phase when the material has the time reversal, parity, and rotation symmetry.

We start from the most general form of the  $4 \times 4$  Hamiltonian

$$H(\mathbf{k}) = R_{\mu\nu}(\mathbf{k})\tau_\mu \otimes \sigma_\nu,$$

where  $R_{\mu\nu}$  is the real function of  $\mathbf{k}$ . We find that the conditions for the time reversal symmetry  $TH(\mathbf{k})T^{-1} = H(-\mathbf{k})$  are

$$\begin{aligned} R_{\mu 0}(-\mathbf{k}) &= R_{\mu 0}(\mathbf{k}), \text{ for } \mu = 0, 1, 3, \\ R_{\mu j}(-\mathbf{k}) &= -R_{\mu j}(\mathbf{k}), \text{ for } \mu = 0, 1, 3, \\ R_{20}(-\mathbf{k}) &= -R_{20}(\mathbf{k}), \\ R_{2j}(-\mathbf{k}) &= R_{2j}(\mathbf{k}), \end{aligned}$$

because the sign of  $\tau_2$  flips due to the complex conjugate operator  $K$  in the time reversal operator(2.15).

Let us consider the parity symmetry  $P$ . Since the parity transformation does not flip the spin, the possible form of the corresponding unitary operator can be written by

$$P = (p_0\tau_0 + p_i\tau_i) \otimes \sigma_0.$$

Since

$$\tau_0 \otimes \sigma_0 = P^2 = (p_0^2 + p_i p_i) \tau_0 \otimes \sigma_0 + 2p_0 p_i \tau_i \otimes \sigma_0,$$

we find the possible parity operator is

$$P = \pm\tau_0 \otimes \sigma_0, \tag{2.16}$$

or

$$P = p_i\tau_i \otimes \sigma_0, \text{ where } |\mathbf{p}| = 1, \tag{2.17}$$

where  $\mathbf{p}$  is real vector. In the latter case, for

$$0 = [T, P] = -2p_2\tau_2 \otimes \sigma_0,$$

we find the parity operator can be written by the parameter  $\theta \in [0, 2\pi]$ ,

$$P = (\cos \theta \tau_3 - \sin \theta \tau_1) \otimes \sigma_0. \quad (2.18)$$

We find that there are two types of the parity transformation: Eq.(2.16) and Eq.(2.18), which is determined by the transformation rule for the orbital degrees of freedom which depends on the material. Correspondingly, the general form of the Hamiltonian with both the time reversal and parity symmetry belongs to the following two types.

In Eq.(2.16) case, the general form of the Hamiltonian with both the time reversal and parity symmetry is

$$H(\mathbf{k}) = R_0(\mathbf{k}) + \sum_{i=1}^5 R_i(\mathbf{k})\Gamma_i,$$

where

$$\Gamma_1 = \tau_1 \otimes \sigma_0, \Gamma_2 = \tau_2 \otimes \sigma_3, \Gamma_3 = \tau_2 \otimes \sigma_2, \Gamma_4 = \tau_2 \otimes \sigma_1, \Gamma_5 = \tau_3 \otimes \sigma_0, \quad (2.19)$$

and  $R_0, R_i$  are the real function. We find all  $R_{0,i}$ s are even functions of the momentum  $\mathbf{k}$ :

$$R_0(-\mathbf{k}) = R_0(\mathbf{k}), R_i(-\mathbf{k}) = R_i(\mathbf{k}).$$

In Eq.(2.18) case, the general form of the Hamiltonian with both the time reversal and parity symmetry is

$$H(\mathbf{k}) = R_0(\mathbf{k}) + \sum_{i=1}^5 R_i(\mathbf{k})\Gamma_i,$$

where

$$\Gamma_1 = \mu_1 \otimes \sigma_3, \Gamma_2 = \mu_2 \otimes \sigma_0, \Gamma_3 = \mu_1 \otimes \sigma_1, \Gamma_4 = \mu_1 \otimes \sigma_2, \Gamma_5 = \mu_3 \otimes \sigma_0, \quad (2.20)$$

where we define

$$\mu_1 = \cos \theta \tau_1 + \sin \theta \tau_3, \mu_2 = \tau_2, \mu_3 = -\sin \theta \tau_1 + \cos \theta \tau_3.$$

We find

$$\begin{aligned} R_0(-\mathbf{k}) &= R_0(\mathbf{k}), R_5(-\mathbf{k}) = R_5(\mathbf{k}), \\ R_i(-\mathbf{k}) &= -R_i(\mathbf{k}), \text{ for } i \neq 5. \end{aligned}$$

In both case, the condition for the band crossing is

$$R_i(\mathbf{k}) = 0,$$

for all  $i$ . When  $R_i$  has a tunable parameter  $m$ , the number of the condition is larger than the number of the parameters. Therefore the valence and conduction band do not cross at the general point in the momentum space. However in Eq.(2.18) case, at the time reversal invariant momentum  $\mathbf{k}_{\text{TRIM}}$ , for instance the zero point of the momentum or the edge of the Brillouin zone, the odd functions of the momentum vanish:

$$R_i(\mathbf{k}_{\text{TRIM}}) = 0, \text{ for } i \neq 5.$$

Therefore the equation of the condition for the band crossing is only

$$R_5(\mathbf{k}_{\text{TRIM}}, M) = 0.$$

Then in this case, we obtain the accidental band crossing at the time reversal invariant momentum, tuning a parameter  $M$ [25]. However the realization of the three dimensional Dirac point by this way requires the very detailed fine tuning of the chemical compositions[28, 29]. This is the case for the Dirac semimetal which appeared in subsection 2.1.

We shall consider  $n$  times rotation symmetry around the  $k_3$ -axis:  $C_n$ , in order to see conditions for the stable Dirac semimetals. The Hamiltonian transform as

$$C_n H(\mathbf{k}) C_n^{-1} = H(R_n \mathbf{k}),$$

where  $R_n$  is the three dimensional  $2\pi/n$  rotation matrix around  $k_3$ -axis  $H(\mathbf{k})|_{k_1=k_2=0}$ :

$$R_n = \begin{pmatrix} \cos \frac{2\pi}{n} & -\sin \frac{2\pi}{n} & 0 \\ \sin \frac{2\pi}{n} & \cos \frac{2\pi}{n} & 0 \\ 0 & 0 & 1 \end{pmatrix}.$$

Since on  $k_3$ -axis (namely  $k_1 = k_2 = 0$ ),  $\mathbf{k}$  is invariant under the rotation, the rotation operator commute with the Hamiltonian on  $k_3$ -axis

$$[C_n, H(\mathbf{k})|_{k_1=k_2=0}] = 0.$$

We can take the basis which simultaneously diagonalize the rotation operator and the Hamiltonian on the  $k_3$ -axis. Then the rotation operator can be written by diagonal form[76]

$$C_n = \begin{pmatrix} u_{A\uparrow} & & & \\ & u_{A\downarrow} & & \\ & & u_{B\uparrow} & \\ & & & u_{B\downarrow} \end{pmatrix} = \begin{pmatrix} \alpha_p & & & \\ & \alpha_q & & \\ & & \alpha_r & \\ & & & \alpha_s \end{pmatrix},$$

where

$$\alpha_p = \exp \left[ \frac{2\pi}{n} i \left( p + \frac{1}{2} \right) \right], \text{ with } p = 0, 1, \dots, n-1.$$

$H(\mathbf{k})|_{k_1=k_2=0}$  has also the diagonal form on this basis, and the four bands are labelled by the eigenvalues of the rotation symmetry  $u_{\tau\sigma}$ . So  $H(\mathbf{k})|_{k_1=k_2=0}$  can be written by

$$H(\mathbf{k})|_{k_1=k_2=0} = R_0(\mathbf{k})| + d(\mathbf{k})\Gamma,$$

where  $d$  is a real function and we find

$$\Gamma = \tau_3, \text{ for } P = \pm\tau_0, \pm\tau_3, \quad (2.21)$$

or

$$\Gamma = \tau_3\sigma_3, \text{ for } P = \pm\tau_1, \quad (2.22)$$

from Eqs.(2.19, 2.20).

In Eq.(2.21) case,  $d$  should be the even function of  $k_3$ , and written as

$$d(k_3) \approx M + \frac{1}{2}t_3k_3^2,$$

in second order in  $k_3$ , where  $M$  and  $t_3$  are parameters independent of  $k_3$ . We find that the Hamiltonian describes either a gapped insulator or a three dimensional Dirac semimetal. Namely, assuming that  $t_3$  has the negative value, if we tune the parameter  $M$ , we can observe the phase transition from the gapped insulator phase in  $M < 0$  to the three dimensional Dirac semimetal phase in  $M > 0$ . Therefore the three dimensional Dirac semimetal with two Dirac points at

$$\mathbf{k} = \left( 0, 0, \pm\sqrt{-\frac{2M}{t_3}} \right),$$

stably exists in  $M > 0$ , without fine tuning of the parameter.  $\text{Na}_3\text{Bi}$ [34, 77] and  $\text{Cd}_3\text{As}_2$ [36, 39, 40], which are confirmed materials that these have the linear dispersion relation at two Dirac points in the experiment, are the examples belonging to this class.

On the other hand, in Eq.(2.22) case,  $d$  should be the odd function of  $k_3$  which can be expanded as

$$d(k_3) \approx vk_3,$$

where  $v$  is a parameter independent of  $k_3$ . In this case, the Hamiltonian describes the Dirac semimetals with single Dirac point at

$$\mathbf{k} = (0, 0, 0).$$

Considering the periodicity of the Brillouin zone, the point

$$\mathbf{k} = (0, 0, \pi),$$

is also Dirac point. Namely, the three dimensional Dirac points stably exists independently of the parameter at the time reversal invariant momentum on the rotation axis.  $\text{BiO}_2$ [30] and the distorted spinels[31], which are theoretically predicted materials that these have the bulk Dirac points, are the examples belonging to this class.

### 3 Magnetotransport Induced by Chiral Anomaly

In this section, we review that the solid state physics has an analogous effect to the chiral anomaly, which breaks the independent conservation of the number of left-handed fermion and right-handed fermion. The imbalance between right- and left-handed Fermi energy arises from the chiral anomaly, with the result that the unusual electric current is generated. Following the discussion in Ref. [1], we start from the macroscopic explanation of the chiral anomaly with a  $1 + 1$  dimensional example.

### 3.1 Macroscopic explanation of the chiral anomaly

We start from the 1 + 1 dimensional right-handed Weyl fermion  $\psi_R$  where the equation is given by right-handed Weyl equation

$$i\partial_0\psi_R(x) = -i\partial_1\psi_R(x).$$

The dispersion relation is given by

$$\epsilon_R(p) = p.$$

When the the uniform electric field

$$E = \partial_0 A^1,$$

is applied, from classical electrodynamics we find

$$\frac{d}{dt}\epsilon_R(p) = \frac{dp}{dt} = eE.$$

The creation rate of the right-handed fermion per unit length is determined by the change of the Fermi energy[Fig:4]. Since the number of states in the unit length is  $\frac{1}{2\pi}$ , the creation rate in unit length is

$$\frac{dN_R}{dt} = \frac{1}{2\pi} \frac{d\mu_R}{dt} = \frac{eE}{2\pi}.$$

This particle creation is the chiral anomaly, and consequently the number of the chiral fermion is not conserved. Similarly for the left-handed Weyl fermion whose dispersion relation is given by

$$\epsilon_L(p) = -p,$$

the creation rate in unit length is derived as

$$\frac{dN_L}{dt} = -\frac{eE}{2\pi}.$$

Then the chiral charge for the Dirac fermion

$$Q_5 = N_R - N_L,$$

is not conserved but obey the anomaly equation:

$$\frac{dQ_5}{dt} = \frac{eE}{\pi}.$$

On the other hand, the vector charge

$$Q = N_R + N_L,$$

is conserved due to the cancelation of the anomaly between left-handed creation and right-handed annihilation

$$\frac{dQ}{dt} = \frac{dN_L}{dt} + \frac{dN_R}{dt} = 0.$$

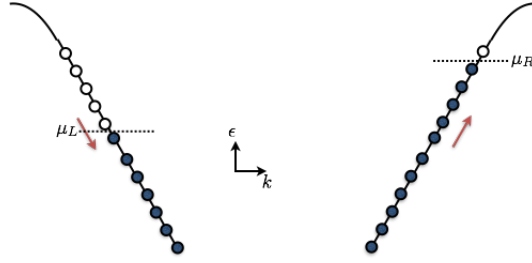


Figure 4: Band structure of the one dimensional Weyl fermion.

In  $3 + 1$  dimensions, we derive the energy level of the right-handed fermion in a constant magnetic field along with the third axis. We take Landau gauge

$$\mathbf{A} = (0, Bx^1, 0), \quad A^0 = 0.$$

The equation for the two component right-handed Weyl field  $\psi_R$  is

$$\left[ i \frac{\partial}{\partial t} - (\mathbf{p} - e\mathbf{A}) \cdot \boldsymbol{\sigma} \right] \psi_R(x) = 0.$$

We introduce the canonical momentum

$$\pi_1 = p_1, \quad \pi_2 = p_2 - eBx^1,$$

where the commutation relation is given by

$$[\pi_1, \pi_2] = ieB.$$

We also define the ladder operator

$$\begin{aligned} a &= \frac{1}{\sqrt{2eB}} (\pi_1 + i\pi_2) \\ a^\dagger &= \frac{1}{\sqrt{2eB}} (\pi_1 - i\pi_2), \end{aligned}$$

and then the commutator is

$$[a, a^\dagger] = 1.$$

The Hamiltonian for the right-handed Weyl fermion under the magnetic field is written in terms of the ladder operator

$$H_R = \begin{pmatrix} p_3 & \sqrt{2eB}a^\dagger \\ \sqrt{2eB}a & -p_3 \end{pmatrix}.$$

Then we find

$$\begin{aligned} H_R^2 &= \begin{pmatrix} p_3^2 + 2eBa^\dagger a & 0 \\ 0 & p_3^2 + 2eBaa^\dagger \end{pmatrix} \\ &= \begin{pmatrix} p_3^2 + 2eBa^\dagger a & 0 \\ 0 & p_3^2 + 2eB(a^\dagger a + 1) \end{pmatrix}. \end{aligned}$$

Therefore we obtain the Landau levels

$$\epsilon_{R,n}(p_3) = \pm\sqrt{p_3^2 + 2eBn}, \text{ for } n > 0.$$

For the zeroth Landau level ( $n = 0$ ), since the lowest Landau state is given by

$$|u_{R,0}\rangle = \begin{pmatrix} |0\rangle \\ 0 \end{pmatrix},$$

where  $|0\rangle$  is the lowest state of the harmonic oscillator, the lowest Landau level for the right-handed fermion is

$$\epsilon_{R,0}(p_3) = +p_3. \quad (3.1)$$

The dispersion relation for right-handed fermion are depicted in [Fig.5].

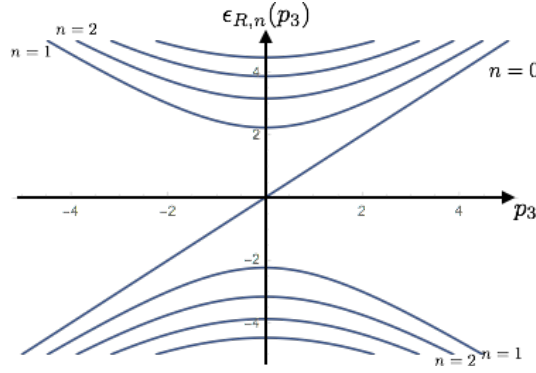


Figure 5: Landau levels for the three dimensional right-handed Weyl fermion under the magnetic field.

Next we consider the constant electric field  $E$  along the third axis, which is parallel to the magnetic field. For the zeroth Landau level the dispersion is the same as the 1+1 dimensional case, and then we can similarly derive the creation rate of the right-handed Weyl fermion. In the case that the electric field is adiabatically applied, the creation of the fermion in the higher Landau levels does not occur. Since the degeneracy of the Landau level in the unit area is given by  $eB/2\pi$ , the creation rate of the right-handed Weyl fermion in unit volume is

$$\frac{dN_R}{dt} = \frac{e^2}{4\pi^2} EB. \quad (3.2)$$

Since the equation for the left-handed Weyl fermion  $\psi_L$  is given by

$$\left[ i\frac{\partial}{\partial t} + (\mathbf{p} - e\mathbf{A}) \cdot \boldsymbol{\sigma} \right] \psi_L(x) = 0,$$

the energy level for the  $n > 0$  states are the same as right-handed one;

$$\epsilon_{L,n}(p_3) = \pm\sqrt{p_3^2 + 2eBn}, \text{ for } n > 0,$$

and zero mode energy is

$$\epsilon_{L,0}(p_3) = -p_3. \quad (3.3)$$

Then we can derive the creation rate of the left-handed Weyl fermion

$$\frac{dN_L}{dt} = -\frac{e^2}{4\pi^2}EB. \quad (3.4)$$

Therefore, the chiral anomaly for the Dirac fermion is

$$\frac{dN_R}{dt} - \frac{dN_L}{dt} = \frac{e^2}{2\pi^2}EB. \quad (3.5)$$

This anomaly equation completely matches with the one derived by quantum exact calculations [4, 5, 78]. The vector charge for the Dirac fermion  $Q = N_R + N_L$  is conserved in 3 + 1 dimension

$$\frac{dQ}{dt} = \frac{dN_R}{dt} + \frac{dN_L}{dt} = 0, \quad (3.6)$$

as well as in 1 + 1 dimension.

## 3.2 Electric current induced by chiral anomaly

In this subsection, we review that the phenomenon analogous to the chiral anomaly appears as the peculiar behavior of the electric conductivity in the gapless system described by the Weyl fermion theory with the Fermi energy  $\mu$ . We consider the case that the valence bands are completely filled and only the conduction band is effective to the electric transport induced by the magnetic field. Without the external field, the cone around the right-handed Weyl point is filled up to the Fermi energy. Then the electron distribution function in the thermodynamical equilibrium is given by the Fermi distribution function

$$f_0(p) = \frac{1}{1 + \exp\left(\frac{\epsilon(p) - \mu}{T}\right)}. \quad (3.7)$$

We consider the case that the magnetic field  $B$  parallel with the electric field is applied, where  $B$  is so strong that only the lowest Landau level is occupied. The dispersion relation is given by Eq.(3.1) for the right-handed fermion and Eq.(3.3) for the left-handed fermion. Since the chiral anomaly carries the fermion from the left-handed cone to the right-handed cone in the momentum space, the deviation from the thermodynamical equilibrium emerges. It can be expressed by the fact that there is difference between the Fermi energy for the fermion at the right-handed Weyl point  $\mu_R$  and one for the fermion at the left-handed Weyl point  $\mu_L$ .

The effect of the chiral anomaly increase the right-handed Fermi energy and decrease the left-handed Fermi energy compared with the Fermi energy without external magnetic field  $\mu$ . To keep the static system the extra fermion in the right-handed Weyl cone due to the chiral anomaly should be scattered back into other states. Change of the number of the right-handed fermion in unit time by the collision is

$$\left(\frac{dN_R}{dt}\right)_{\text{coll}} = - \int d^3\mathbf{p}d^3\mathbf{p}' f_R(\mathbf{p})(1 - f_L(\mathbf{p}'))W(\mathbf{p} \rightarrow \mathbf{p}') + \int d^3\mathbf{p}d^3\mathbf{p}' f_L(\mathbf{p}')(1 - f_R(\mathbf{p}))W(\mathbf{p}' \rightarrow \mathbf{p}),$$

where  $f_{L/R}$  is the Fermi distribution function (3.7) with the Fermi energy  $\mu_{L/R}$ , respectively, and  $W(\mathbf{p} \rightarrow \mathbf{p}')$  is the transfer probability in unit time. Setting the deviation of the distribution function of the right- and left-handed fermion from the equilibrium as  $\delta f_{R/L}$ , respectively, we expand above equation in the first order of  $\delta f_{R/L}$ ,

$$\begin{aligned} \left(\frac{dN_R}{dt}\right)_{\text{coll}} = & - \int d^3\mathbf{p}d^3\mathbf{p}'W(\mathbf{p} \rightarrow \mathbf{p}')[\delta f_R(\mathbf{p})(1 - f_0(\mathbf{p}')) - f_0(\mathbf{p})\delta f_L(\mathbf{p}')] \\ & + \int d^3\mathbf{p}d^3\mathbf{p}'W(\mathbf{p}' \rightarrow \mathbf{p})[\delta f_L(\mathbf{p}')(1 - f_0(\mathbf{p})) - f_0(\mathbf{p}')\delta f_R(\mathbf{p})]. \end{aligned}$$

From the energy conservation law we find that the distribution function in the equilibrium is unchanged ( $f_0(\mathbf{p}') = f_0(\mathbf{p})$ ). Since the transfer probability depends only on the relative angle between  $\mathbf{p}$  and  $\mathbf{p}'$ , we find also that the transfer probability is symmetric ( $W(\mathbf{p}' \rightarrow \mathbf{p}) = W(\mathbf{p} \rightarrow \mathbf{p}')$ ). Then we find

$$\left(\frac{dN_R}{dt}\right)_{\text{coll}} = - \int d^3\mathbf{p}d^3\mathbf{p}'W(\mathbf{p} \rightarrow \mathbf{p}')[\delta f_R(\mathbf{p}) - \delta f_L(\mathbf{p}')].$$

From the vector charge conservation law (3.6), the rise of the right-handed Fermi energy is the same as the fall of the left-handed Fermi energy

$$\mu = \frac{\mu_R + \mu_L}{2}. \quad (3.8)$$

If the deviation from the Fermi energy in the equilibrium is very small, we find

$$\delta f_R(\mathbf{p}) = -\delta f_L(\mathbf{p}'),$$

and so the collision term is

$$\left(\frac{dN_R}{dt}\right)_{\text{coll}} = -2 \int d^3\mathbf{p}d^3\mathbf{p}'W(\mathbf{p} \rightarrow \mathbf{p}')\delta f_R(\mathbf{p}). \quad (3.9)$$

Here we define a relaxation time  $\tau$  by

$$\left(\frac{dN_R}{dt}\right)_{\text{coll}} = -\frac{N_R - N_R^0}{\tau}, \quad (3.10)$$

where

$$N_R = \int d^3\mathbf{p}f_R(\mathbf{p}), \text{ and } N_0 = \int d^3\mathbf{p}f_0(\mathbf{p}).$$

Therefore we can derive the relaxation time if the transition probability from the right-handed cone into the left-handed cone  $W(\mathbf{p} \rightarrow \mathbf{p}')$  is calculated.

The generation of the electric current associated with the chiral anomaly is shown by the discussion of the energy conservation. From Eq.(3.2, 3.4)  $\frac{e^2EB}{4\pi^2}$  of the electrons move from the left-handed cone to the right-handed cone per unit time and unit volume due to the chiral anomaly. Since the right-handed Fermi energy is larger than the left-handed Fermi energy, the energy  $\frac{e^2EB}{4\pi^2}(\mu_R - \mu_L)$  is necessary to carry the electron. This energy is supplied

from the electric current  $J$  and the external electric field  $E$ , and so the size of the current is determined by the energy balance

$$EJ = \frac{e^2 EB}{4\pi^2}(\mu_R - \mu_L). \quad (3.11)$$

At zero temperature, since the distribution function in the right-handed cone is

$$f_R(\epsilon) = \theta(\mu_R - \epsilon(p_3)) = \theta(\mu_R - p_3),$$

then the number of the right-handed fermion per unit volume is

$$N_R = \frac{eB}{2\pi} \int^{\mu_R} \frac{dp_3}{2\pi},$$

where  $\frac{eB}{2\pi}$  is the degeneracy of the Landau level. When the difference of the right-handed Fermi energy from the Fermi energy in zero magnetic field is very small, we obtain

$$N_R \approx N_0 + \frac{eB}{4\pi^2} \frac{\mu_R - \mu_L}{2},$$

where we use Eq.(3.8). Therefore the collision term (3.10) becomes

$$\left( \frac{dN_R}{dt} \right)_{\text{coll}} = -\frac{eB}{4\pi^2} \frac{\mu_R - \mu_L}{2\tau}.$$

Substituting this equation and the drift term (3.2) into the static Boltzmann equation

$$\left( \frac{dN_R}{dt} \right)_{\text{drift}} = - \left( \frac{dN_R}{dt} \right)_{\text{coll}},$$

we obtain

$$\mu_R - \mu_L = 2eE\tau.$$

Finally, from Eq.(3.11) we obtain the current associated with the chiral anomaly

$$J = \frac{2e^3 EB\tau}{4\pi^2}.$$

This electric current coming from the imbalance between the right- and left-handed Fermi energy is the macroscopic manifestation of the chiral anomaly, and is called a chiral magnetic effect. It can be observed in various system which possesses the relativistic fermion such as the Weyl or Dirac semimetals.

The negative magnetoresistance related to the chiral anomaly in Weyl semimetals is theoretically discussed in many papers [64, 65, 66, 79, 80, 81]. The relaxation of the chirality imbalance is only roughly discussed or just assumed to be large in these papers. The prediction for the electric current induced by the chiral anomaly required the estimation of the relaxation time.

### 3.3 Previous study for relaxation time

The relaxation time defined by Eq.(3.10) is determined by the transfer probability, and it was calculated for several cases. In this subsection, we show these previous studies and clarify what is already known and what should be studied about the relaxation time.

In Ref. [2], the magnetic field effect on the scattering of the electron in semiconductor was studied in non-relativistic theory without the chiral anomaly consideration. They estimated the longitudinal magnetoresistance under the strong magnetic field where all the electrons in the conduction band is in the lowest Landau level. They calculate the relaxation time for the scattering by phonons and ionized impurities in the low temperature case  $T \ll \epsilon_F$  and in the high temperature case  $\epsilon_F \ll T$ . They find that while for the acoustic phonon scattering a magnetoresistance is always positive, for the ionized impurity scattering a negative magnetoresistance is expected.

In Ref. [60], they have investigated the angle dependence of the magnetoresistance in the quantum limit where one can ignore all but the lowest Landau level, extending the previous study of the long range impurity scattering [82, 58, 83]. They have found that the relaxation time for inter-cone transition exponentially decreases when the magnetic field is tilted from the direction along with the momentum separation of the two Weyl nodes in strong magnetic field region. They also shown that under the weak magnetic field, inter-cone transition rate is independent of the angle of the magnetic field.

The magnetoconductivity induced by the chiral anomaly by means of the chiral magnetic effect in strongly coupled holographic models is studied in Ref. [84, 85, 86]. They introduce two sources to relax the chirality imbalance in the holographic system. One is a mass for the  $U_A(1)$  gauge field so that there is no  $U_A(1)$  gauge symmetry in the bulk anymore. The other is an axially charged scalar field which is explicitly breaks  $U_A(1)$  symmetry in bulk. They report that the chirality imbalance relaxation time grows linearly with magnetic field in the large magnetic field regime.

Due to the Berry phase, for the Weyl semimetals the weak anti-localization effect arises [54, 55], which is suppression mechanism of the back scattering in zero magnetic field. The interference term between the process from the state with momentum  $\mathbf{k}$  to the state with momentum  $-\mathbf{k}$  through the multiple scattering and its time reversed process get the Berry phase  $\pm\pi$  for the Weyl node with the monopole charge  $\pm 1$ . Due to the Berry phase, the quantum correction to the probability of the back scattering get a minus sign. Therefore, since this effect disappears under the magnetic field which breaks the time reversal symmetry, the magnetoconductivity becomes negative when magnetic field is weakly applied.

The Weyl semimetal has the features that the band gap closes at two points and that it has the topological surface states. Many of papers discussing the magnetotransport of the Weyl semimetal consider the bulk theory with the periodic boundary condition. In Ref. [57], the magnetoconductivity in the Weyl semimetal with the surface boundary condition has been studied under the strong magnetic field where only the lowest Landau level contribute to the transport phenomenon. They have reported that the magnetoconductivity increases proportional to the magnetic field due to the inter-cone transition mediated through the surface states.

The magnetotransport under strong magnetic field in the three dimensional Weyl semimetal has been investigated in Ref. [59]. They have theoretically considered not only the model of the single Weyl semimetal with the monopole charge  $\mathcal{N}$  is one, but also the model of the

generalized Weyl semimetals with the monopole charge two and three, though the multi-monopole Weyl semimetals have not been realized in the experiment. The  $\mathcal{N}$ -monopole Weyl semimetals have exactly  $\mathcal{N}$  number of the lowest Landau level under the strong magnetic field, and so the anomaly equation for the multi-monopole Weyl semimetal becomes multiplied by  $\mathcal{N}$

$$\frac{dN_R}{dt} - \frac{dN_L}{dt} = \mathcal{N} \frac{e^2}{2\pi^2} EB.$$

Using the linearized Boltzmann equation, they have obtained the magnetic field dependence of the relaxation time both for the Gaussian and Coulomb impurities in the Weyl semimetal with the monopole charge one, two, and three which are all the possible number of the monopole charge in the three dimensional Weyl semimetal. They have shown that the longitudinal magnetoconductivity is the general property of the three dimensional system with the impurity scattering under the strong magnetic field without the discussion about the chiral anomaly. They have found that there is always positive longitudinal magnetoconductivity (namely negative longitudinal magnetoresistance) in the presence of both the Gaussian and Coulomb impurities, using linearized Boltzmann equation. In the presence of only the Gaussian impurities, the longitudinal magnetoconductivity increase linearly in  $B$ , while in the presence of only the screened Coulomb impurities, the magnetoconductivity depends on  $B^2$  in a strong magnetic field limit. They have also reported that in the multi-monopole Weyl semimetals ( $\mathcal{N} = 2, 3$ ) the magnetic field dependence of the longitudinal magnetoconductivity becomes non-linear form depending the angle of the magnetic field.

In Ref. [61] they have presented the dependence of the longitudinal and the transverse conductivity of Dirac Semimetals as a function of magnetic field and effective coupling constant by the lattice Monte Carlo simulation using the staggered fermion. They have investigated the effect of the electron-electron scattering effect on the magnetoconductivity not only for massless Dirac semimetal phase, but also onset of the insulator phase and deep in the insulator phase. In the semimetal phase, they have observed the positive longitudinal magnetoconductivity and the negative transverse magnetoconductivity. It has been noticed that there are two regimes of the dependence of the longitudinal conductivity on the magnetic field. For small values of magnetic field the longitudinal magnetoconductivity is quadratically increasing function, while for larger values of magnetic field it is linearly increasing function.

We would like to predict some universal feature of the magnetoconductivity which is model independent by relativistic calculation. Since the experiment measures the magnetoconductivity of semimetals for a wide range of the magnetic field strength, it is needed to predict the relaxation time for electrons in the Dirac or Weyl semimetals with the magnetic field both in and away from the quantum limit. On the other hand, even in the same material  $\text{Cd}_3\text{As}_2$ , when its carrier density is very high, the behavior of the observed longitudinal magnetoresistance is not negative, but the usual Shubnikov de Haas oscillation [62]. This experiment indicates that when the lowest Landau level is hidden under the Fermi energy due to the too weak magnetic field or the relatively high Fermi energy, the negative magnetoresistance due to the chiral anomaly does not emerge. We would like to address the middle range between the ultra high Fermi energy case and the case in the quantum limit. Besides, since the realization of the unstable Dirac semimetals requires the very detailed fine tuning of the parameter, the Dirac semimetals used in the experiments [43, 44] have the possibility of the small gap opening. Even in the stable Dirac semimetals, since the Dirac semimetals

used in the experiments [32, 33] may have very small mass gap due to the deviation of the magnetic field direction from the symmetric direction which protect the stable Dirac nodes. Therefore we would also like to estimate the effect of the mass gap of the Dirac fermion to the magnetoconductivity. From the next section, we give the details of our calculation and the result for this purpose.

## Part II

# Calculation of Relaxation Time

In this part, we give details of our calculation following the published paper[3]. The preliminary discussions are given in the proceedings[87, 88].

## 4 Massive Dirac Fermion and Transport Theory

In this section, revisiting the theory for the massive Dirac fermion under the magnetic field and the basics of the transport theory, we derive the relation between the electric current and the relaxation times when both the electric field  $\mathbf{E}$  and the magnetic field  $\mathbf{B}$  are applied along the third axis. Due to the magnetic field, the electron states in the first and second directions form Landau levels. In the case that one is interested in the low energy physics under the strong magnetic field, the effective system becomes a 1 + 1 dimensional electron system since only the lowest Landau level contribute to the physics. When the electric field in the third direction is applied, the electron gets the drifting force and the electric current flows. Due to the scattering from impurities, phonon excitations and other electrons, the momentum of the electrons are flipped and the current becomes static as a result of the balance between the drift and the relaxation by the scatterings.

In usual discussions, only the Weyl or Dirac semimetal in the quantum limit are considered. In this case, due to the helicity conservation, only the inter-cone transition takes place as shown in Fig.6. In our study, we generalize the situation and consider the electron system with a small mass gap and the magnetic field both in and away from the quantum limit using the low energy effective theory.

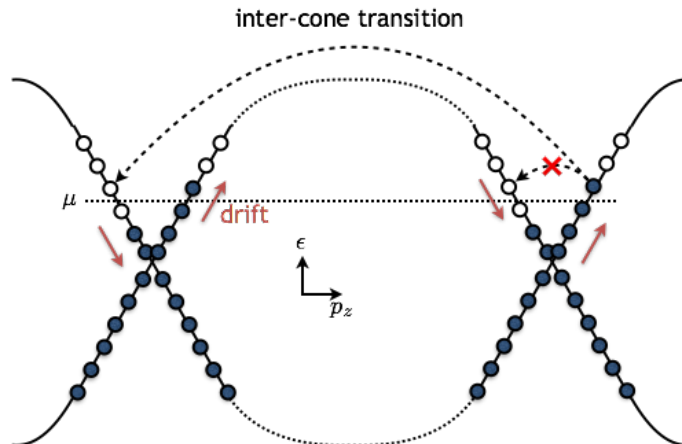


Figure 6: In the inter-cone transition the fermion is scattered into the other cone. Since the inter-cone transition is highly dependent on its modeling, it is difficult to give a universal prediction.

The low energy effective theory description using the relativistic fermion is valid provided that one considers low energy phenomena which takes place within the Dirac cone in mind. However, the transition between two different Dirac cones (inter-cone transition

[Fig.6]) cannot be described by the low energy theory since the transition amplitude receives non-negligible contributions from the integral over the entire momentum space. In the following, we assume that there is always a inter-cone transition which can only be predicted by the full theory, but the relaxation time after the onset of the intra-cone transition [Fig.7] can be well described by the low energy effective theory. In general, if the separation of Dirac points are sufficiently large compared with the Fermi energy, the intra-cone transition[Fig.7] dominates over the inter-cone transition. So we consider the case that the inter-cone transition effect is much smaller than the intra-cone transition effect.

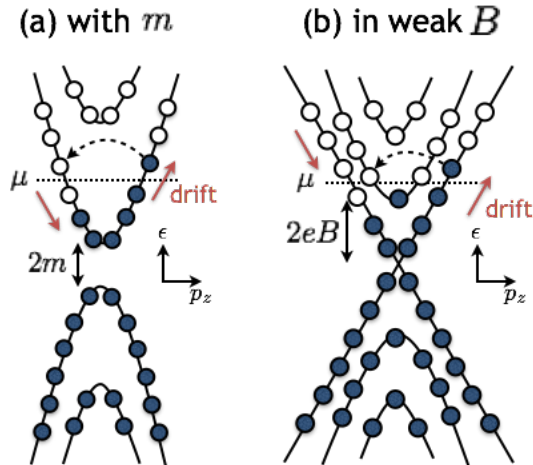


Figure 7: The mechanisms of the intra-cone transition due to (a)the mass and (b)the first excited states in a weak magnetic field region. The effect of the intra-cone transition can be estimated in the low energy effective theory.

We introduce a small mass in order to include a mass gap due to a mechanical strain or deviation of the parameter from the critical point. Examples of strain-induced mass gap is studied for several materials in Ref.[32, 40, 41, 42].

#### 4.1 Massive Dirac fermion in the magnetic field

In this subsection we solve the massive Dirac equation under the magnetic field for preparation for the calculation of the mass dependence of the relaxation time.

We solve the massive Dirac equation derived from the action

$$S = \int d^4x \bar{\psi}(x) [i\mathcal{D} - m] \psi(x), \quad (4.1)$$

under a magnetic field, where

$$\mathcal{D} = \gamma^\mu D_\mu = \gamma^\mu (\partial_\mu - ieA_\mu).$$

Here,  $\gamma$  matrices are taken to be Weyl representation:

$$\gamma^i = i\tau_2 \otimes \sigma^i = \begin{pmatrix} 0 & \sigma^i \\ -\sigma^i & 0 \end{pmatrix}, \quad \gamma^0 = \tau_1 \otimes \sigma^0 = \begin{pmatrix} 0 & \sigma^0 \\ \sigma^0 & 0 \end{pmatrix}. \quad (4.2)$$

We consider the Dirac fermion with mass  $m \neq 0$ , which obeys the Dirac equation:

$$[i\mathcal{D} - m]\psi(x) = 0. \quad (4.3)$$

Since we consider a constant background magnetic field along the third axis, the gauge is taken so that the vector potential corresponding the magnetic field whose magnitude is  $B$  is

$$\mathbf{A} = (0, Bx^1, 0). \quad (4.4)$$

In this gauge, the momentum  $p_2$  is a good quantum number to label the states in order to distinguish the degenerate states in  $n$ -th Landau level. Multiplying  $\gamma^0$  to the Dirac equation from left,

$$[i\partial_0 + i\gamma^0\gamma^i D_i - m\gamma^0]\psi(x) = 0. \quad (4.5)$$

Introducing the canonical momentum

$$\pi_1 = p_1, \quad \pi_2 = p_2 - eBx^1,$$

where the commutation relation is given by

$$[\pi_1, \pi_2] = ieB.$$

We also define the ladder operator

$$\begin{aligned} a &= \frac{1}{\sqrt{2eB}}(\pi_1 + i\pi_2) \\ a^\dagger &= \frac{1}{\sqrt{2eB}}(\pi_1 - i\pi_2), \end{aligned}$$

and then the commutator is

$$[a, a^\dagger] = 1.$$

The Hamiltonian for the massive Dirac fermion under the magnetic field is written in terms of the ladder operator

$$H = -\tau_3 \otimes \begin{pmatrix} p_3 & \sqrt{2eB}a^\dagger \\ \sqrt{2eB}a & -p_3 \end{pmatrix} + m\tau_1 \otimes \sigma^0.$$

Then we find

$$H^2 = \tau_0 \otimes \begin{pmatrix} m^2 + p_3^2 + 2eBa^\dagger a & 0 \\ 0 & m^2 + p_3^2 + 2eB(a^\dagger a + 1) \end{pmatrix}.$$

Therefore, the energy levels are given by Landau levels

$$\epsilon_{n,\sigma_3}(p_3) = \pm \sqrt{2eB \left( n + \frac{1}{2} \right) + p_3^2 + m^2 - eB\sigma_3}, \quad (4.6)$$

where each states are degenerated in  $p_2$  space. Note that the states with  $(n, \sigma_3 = -1)$  and  $(n + 1, \sigma_3 = +1)$  are degenerated except for the lowest Landau level ( $n = 0, \sigma_3 = +1$ ). Negative energy states do not contribute to the scattering, because these are always occupied. The energy eigenstate is given by the four component spinor

$$\begin{aligned} |n, \sigma_3 = +1; p_2, p_3\rangle &= \frac{\epsilon_{n, \sigma_3}(p_3) + H}{2\sqrt{\epsilon_{n, \sigma_3}(p_3)(\epsilon_{n, \sigma_3}(p_3) + m)}} \begin{pmatrix} |n, p_2, p_3\rangle \\ 0 \\ |n, p_2, p_3\rangle \\ 0 \end{pmatrix}, \\ |n, \sigma_3 = -1; p_2, p_3\rangle &= \frac{\epsilon_{n, \sigma_3}(p_3) + H}{2\sqrt{\epsilon_{n, \sigma_3}(p_3)(\epsilon_{n, \sigma_3}(p_3) + m)}} \begin{pmatrix} 0 \\ |n, p_2, p_3\rangle \\ 0 \\ |n, p_2, p_3\rangle \end{pmatrix}, \end{aligned}$$

where  $\frac{1}{2\sqrt{\epsilon(\epsilon+m)}}$  is the normalization constant determined by the normalization condition

$$\langle n', \sigma'_3; p'_2, p'_3 | n, \sigma_3; p_2, p_3 \rangle = (2\pi)^2 \delta(p_2 - p'_2) \delta(p_3 - p'_3) \delta_{n, n'} \delta_{\sigma_3, \sigma'_3}. \quad (4.7)$$

$|n, p_2, p_3\rangle$  is the  $n$ -th state of the harmonic oscillator defined by

$$|n, p_2, p_3\rangle = \frac{(a^\dagger)^n}{\sqrt{n!}} |0, p_2, p_3\rangle,$$

where  $|0, p_2, p_3\rangle$  is zeroth state of the harmonic oscillator defined by

$$a|0, p_2, p_3\rangle = 0.$$

In coordinate representation,  $|0, p_2, p_3\rangle$  is given by

$$\langle x | 0, p_2, p_3 \rangle = \left( \frac{eB}{\pi} \right)^{1/4} e^{ip_2 x^2 + p_3 x^3} \exp \left[ -\frac{eB}{2} \left( x^1 - \frac{p_2}{eB} \right)^2 \right].$$

## 4.2 Basics of the transport theory

In this subsection, we revisit the basics of the transport theory in the case that the magnetic field is applied along with the electric field. Considering here the case that the multiple bands cross the Fermi energy, we derive the relation between the electric current and the relaxation times at each states.

Consider a probability function  $f(n, \mathbf{p}, t)$  for the electron with the the second and third direction momentum  $\mathbf{p} = (p_2, p_3)$  in the  $n$ -th Landau level. Applying a weak electric field in the same direction as the magnetic field

$$\mathbf{E} = (0, 0, E), \quad (4.8)$$

the Boltzmann equation is given by

$$\frac{\partial}{\partial t} f(n, \mathbf{p}, t) - eE \frac{\partial}{\partial p_3} f(n, \mathbf{p}, t) = \left( \frac{\partial}{\partial t} f(n, \mathbf{p}, t) \right)_{\text{coll}}, \quad (4.9)$$

where the second term of the left hand side is the drift term and the right hand side is the collision term. The collision term is defined as

$$\begin{aligned} \left( \frac{\partial}{\partial t} f(n, \mathbf{p}, t) \right)_{\text{coll}} &= - \sum_{n'} \int_{\text{BZ}} \frac{d^2 \mathbf{p}'}{(2\pi)^2} f(n, \mathbf{p}, t) W(n, \mathbf{p}, \rightarrow n', \mathbf{p}') (1 - f(n', \mathbf{p}', t)) \\ &+ \sum_{n'} \int_{\text{BZ}} \frac{d^2 \mathbf{p}'}{(2\pi)^2} f(n', \mathbf{p}', t) W(n', \mathbf{p}', \rightarrow n, \mathbf{p}) (1 - f(n, \mathbf{p}, t)), \end{aligned} \quad (4.10)$$

where  $W$  is the transfer probability in unit time.

Due to the very weak electric field which can be treated as a perturbation, the distribution function is slightly deviated from the equilibrium and can be described as

$$f(n, \mathbf{p}, t) = f_0(\epsilon) + \delta f(n, \mathbf{p}, t), \quad (4.11)$$

where  $f_0$  is the probability distribution function in the equilibrium with no electric field and  $\delta f$  is the tiny deviation from the equilibrium of  $\mathcal{O}(eE)$  for the  $n$ -th Landau level.  $\epsilon$  is the energy of the electron.

From the Fermi's golden rule, the energy is conserved before and after the transition so that the distribution function in equilibrium does not change between the transition

$$f_0(\epsilon) = f_0(\epsilon').$$

Since the transfer probability depends only on the relative angle between the momentum  $\mathbf{p}$  and  $\mathbf{p}'$ , we also find the transfer probability is symmetric. Assuming a small deviation from the equilibrium, the right hand side of the definition of the collision term becomes

$$\left( \frac{\partial}{\partial t} f(n, \mathbf{p}, t) \right)_{\text{coll}} = - \sum_{n'} \int_{\text{BZ}} \frac{d^2 \mathbf{p}'}{(2\pi)^2} W(n, \mathbf{p} \rightarrow n', \mathbf{p}') (\delta f(n, \mathbf{p}, t) - \delta f(n', \mathbf{p}', t)), \quad (4.12)$$

up to higher order terms in  $\delta f$ .

To solve the Boltzmann equation, one often makes the relaxation time approximation, which assume that the probability distribution function exponentially get back into the thermodynamical equilibrium in relaxation time  $\tau(n, \mathbf{p})$  due to the scattering effect:  $\delta f \propto e^{-t/\tau}$ . Then the collision term can be written as

$$\left( \frac{\partial}{\partial t} f(n, \mathbf{p}, t) \right)_{\text{coll}} =: - \frac{\delta f(n, \mathbf{p}, t)}{\tau(n, \mathbf{p})}. \quad (4.13)$$

Substituting this equation into Eq.(4.9), the static solution of the Boltzmann equation is

$$f(n, \mathbf{p}) = f_0(\epsilon) + eE\tau(n, \mathbf{p}) \frac{\partial f_0(\epsilon)}{\partial p_3} + \mathcal{O}(E^2). \quad (4.14)$$

Thus, the deviation from the equilibrium in the lowest order in  $eE$  is

$$\delta f(n, \mathbf{p}) = eE\tau(n, \mathbf{p}) \frac{\partial f_0(\epsilon)}{\partial p_3} = eE\tau(n, \mathbf{p}) \frac{\partial \epsilon(n, \mathbf{p})}{\partial p_3} f_0'(\epsilon). \quad (4.15)$$

Substituting Eq.(4.13), (4.15) into the equation for the definition of the collision term (4.12) and considering an energy conservation law, the equation to determine the relaxation time  $\tau$  is obtained as

$$\frac{\partial \epsilon(n, \mathbf{p})}{\partial p_3} = \sum_{n'} \int_{\text{BZ}} \frac{d^2 \mathbf{p}'}{(2\pi)^2} W(n, \mathbf{p} \rightarrow n', \mathbf{p}') \left( \tau(n, \mathbf{p}) \frac{\partial \epsilon(n, \mathbf{p})}{\partial p_3} - \tau(n', \mathbf{p}') \frac{\partial \epsilon(n', \mathbf{p}')}{\partial p'_3} \right). \quad (4.16)$$

Only the states around the Dirac points contribute to the low energy physics. Therefore, we can replace the momentum integral in the Brillouin zone:

$$\int_{\text{BZ}} \frac{d^2 p}{(2\pi)^2} F(\mathbf{p}), \quad (4.17)$$

with the low energy momentum integral and the sum of cones labeled by  $A$

$$\sum_A \int_{\text{low energy}} \frac{d^2 q}{(2\pi)^2} F(\mathbf{p}_A + \mathbf{q}), \quad (4.18)$$

where  $F(\mathbf{p})$  is any function of  $\mathbf{p}$ , and  $\mathbf{p}_A$  is the momentum on the Dirac cone labeled by  $A$ . Then Eq.(4.16) can be rewritten by

$$\begin{aligned} & \frac{\partial \epsilon(n, \mathbf{p}_A + \mathbf{q})}{\partial q_3} \\ = & \sum_{n', A'} \int_{\text{low energy}} \frac{d^2 \mathbf{q}'}{(2\pi)^2} W(n, \mathbf{p}_A + \mathbf{q} \rightarrow n', \mathbf{p}_{A'} + \mathbf{q}') \\ \times & \left( \tau(n, \mathbf{p}_A + \mathbf{q}) \frac{\partial \epsilon(n, \mathbf{p}_A + \mathbf{q})}{\partial q_3} - \tau(n', \mathbf{p}_{A'} + \mathbf{q}') \frac{\partial \epsilon(n', \mathbf{p}_{A'} + \mathbf{q}')}{\partial q'_3} \right). \end{aligned} \quad (4.19)$$

In the case that  $A = A'$ , it denotes the contribution from the intra-cone transition which will be estimated in this paper. In the case that  $A \neq A'$ , it denotes the contribution from the inter-cone transition which is a model- and situation-dependent quantity.

In the following, we consider the intra-cone transition. Then we omit the cone labeling  $A$  and the indication 'low energy' in the integral.  $\mathbf{p}$  is taken to be the momentum around the Dirac point  $\mathbf{p}_A$ . From the energy eigenvalue (4.6), Eq.(4.16) is simplified as

$$p_3 = \sum_{n'} \int \frac{d^2 \mathbf{p}'}{(2\pi)^2} W(n, \mathbf{p} \rightarrow n', \mathbf{p}') (\tau(n, \mathbf{p}) p_3 - \tau(n', \mathbf{p}') p'_3), \quad (4.20)$$

where  $n$  is a label for the Landau level.

The electric current density in the the third direction is given by

$$J = -e \sum_n \int \frac{d^2 \mathbf{p}}{(2\pi)^2} \frac{\partial \epsilon(n, \mathbf{p})}{\partial p_3} f(n, \mathbf{p}). \quad (4.21)$$

From Eq.(4.14), the expression of the current becomes

$$J = \sum_n \int \frac{d^2 p}{(2\pi)^2} (-e) \frac{\partial \epsilon(n, \mathbf{p})}{\partial p_3} \left( f_0(\epsilon) + eE\tau(n, \mathbf{p}) \frac{\partial f_0(\epsilon)}{\partial p_3} \right). \quad (4.22)$$

Due to the translation invariance, it turns out that the relaxation time does not depend on the initial momentum  $p_y$ , and  $p_y$  can be regarded as just a label of the degenerate states. Since the probability distribution function is given by the step function:  $f_0 = \theta(\mu - \epsilon)$  at zero temperature, it becomes

$$\begin{aligned} f(n, \mathbf{p}) &= \theta(\mu - \epsilon) + eE\tau(n, p_3)\frac{\partial}{\partial p_3}\theta(\mu - \epsilon) \\ &= \theta(\mu - \epsilon) - eE\tau(n, p_3)\delta(\mu - \epsilon)\frac{\partial \epsilon}{\partial p_3}. \end{aligned}$$

Then the size of the current is expressed as

$$J = \frac{-e^3BE}{(2\pi)^2\mu} \sum_n \sum_{P_*} |P_*| \tau(n, P_*), \quad (4.23)$$

where  $P_*$  is defined as the values of  $p_3$  which satisfy  $\epsilon(p_3) = \mu$ .

## 5 Relaxation time for massive fermion in strong magnetic field

In this section, we give the details of the calculation of the scattering amplitude and the relaxation time for a relativistic fermion with a small mass in the strong magnetic field region. Although there are the inter-cone transition contributions to the relaxation time in the Dirac semimetals, we only consider the scattering within the cone in this section. In the strong magnetic field region only the lowest Landau level  $(n, \sigma_3) = (0, +1)$  contribute to the scattering. Since we consider only this state, let us omit the label  $(n, \sigma_3)$  in this section. This approximation is valid in the limit  $eB \rightarrow \infty$ .

We find  $P_*$  in Eq.(4.23) is given by

$$P_1 = \sqrt{\mu^2 - m^2}, \quad (5.1)$$

or  $-P_1$ . At zero temperature, only these two states at the Fermi level contribute to the scattering. Then the size of the current can be written as

$$J = \frac{-e^3BE}{(2\pi)^2\mu} P_1 (\tau(P_1) + \tau(-P_1)). \quad (5.2)$$

Since the probability distributions  $f$  and  $f_0$  are normalized to unity, their difference satisfies

$$\int \frac{d^2p}{(2\pi)^2} \delta f(p_2, p_3) = 0,$$

from which one obtains using Eq.(4.15)

$$\tau(P_1) - \tau(-P_1) = 0. \quad (5.3)$$

From the Fermi's golden rule, the energy is conserved before and after the transition so that the probability can be written as

$$W(p_2, p_3 \rightarrow, p'_2, p'_3) \equiv 2\pi\delta(\epsilon(p_3) - \epsilon(p'_3))\overline{W}(p_2, p_3 \rightarrow, p'_2, p'_3). \quad (5.4)$$

We obtain from Eq.(4.20)

$$\begin{aligned} P_1 &= \int \frac{d^2\mathbf{P}'}{(2\pi)^2} 2\pi\delta(\epsilon(P_1) - \epsilon(p'_3))\overline{W}(p_2, P_1 \rightarrow, p'_2, p'_3)(\tau(P_1)P_1 - \tau(p'_3)p'_3) \\ &= 2\mu\tau(P_1) \int \frac{dp'_2}{2\pi} \overline{W}(p_2, P_1 \rightarrow p'_2, -P_1). \end{aligned} \quad (5.5)$$

The transition rate per unit time is given by

$$\overline{W}(p_2, p_3 \rightarrow p'_2, p'_3) = \sum_{\mathbf{R}} |\langle p'_2, p'_3 | v(\hat{\mathbf{r}} - \mathbf{R}) | p_2, p_3 \rangle|^2, \quad (5.6)$$

where  $\mathbf{R}$  stands for the position of the impurity, and  $\hat{\mathbf{r}}$  is the position operator for the fermions. We consider the interaction between the fermion and the charged impurity given by the screened Coulomb potential:

$$v(\mathbf{x}) = \frac{e^2 \exp(-|\mathbf{x}|/r_s)}{\kappa |\mathbf{x}|}, \quad (5.7)$$

where  $r_s$  is the screening length and  $\kappa$  is the dielectric constant. We ignore the interference effect between the states scattered by different impurities. The Fourier transformed screened Coulomb potential is given by

$$v(\mathbf{x} - \mathbf{R}) = \pm \frac{4\pi e^2}{\kappa} \frac{1}{V} \sum_{\mathbf{q}} \frac{e^{i\mathbf{q}\cdot(\mathbf{x}-\mathbf{R})}}{q^2 + 1/r_s^2}.$$

After some calculation we obtain the matrix element

$$\begin{aligned} \langle p'_2, p'_3 | e^{i\mathbf{q}\cdot\mathbf{x}} | p_2, p_3 \rangle &= \int d^3x e^{i\mathbf{q}\cdot\mathbf{x}} \langle p'_2, p'_3 | \mathbf{x} \rangle \langle \mathbf{x} | p_2, p_3 \rangle \\ &= (2\pi)^2 \delta(p_2 - p'_2 - q_y) \delta(p_3 - p'_3 - q_z) \frac{(\epsilon(p'_3) + m)(\epsilon(p_3) + m) + p'_3 p_3}{2\sqrt{\epsilon(p_3)\epsilon(p'_3)(\epsilon(p_3) + m)(\epsilon(p'_3) + m)}} \\ &\quad \times \exp\left[-\frac{1}{4eB} \{q_x^2 + q_y^2 + 2q_x i(p'_2 + p_2)\}\right]. \end{aligned}$$

Assuming that the impurities are distributed uniformly with the density  $N_I$ , we can calculate  $\overline{W}$  analytically

$$\begin{aligned} \overline{W}(p_2, p_3 \rightarrow p'_2, p'_3) &= \left(\frac{4\pi e^2}{\kappa V}\right)^2 \sum_{\mathbf{R}} \left| \sum_{\mathbf{q}} \frac{\langle p'_2, p'_3 | e^{i\mathbf{q}\cdot(\mathbf{r}-\mathbf{R})} | p_2, p_3 \rangle}{q^2 + 1/r_s^2} \right|^2 \\ &= \left(\frac{4\pi e^2}{\kappa}\right)^2 \frac{N_I}{V} \frac{[(\epsilon(p'_3) + m)(\epsilon(p_3) + m) + p'_3 p_3]^2}{4\epsilon(p_3)\epsilon(p'_3)(\epsilon(p_3) + m)(\epsilon(p'_3) + m)} \\ &\quad \times \sum_{q_1} \frac{\exp\left[-\frac{1}{2eB} \{q_1^2 + (p_2 - p'_2)^2\}\right]}{[q_1^2 + (p_2 - p'_2)^2 + (p_3 - p'_3)^2 + 1/r_s^2]^2}. \end{aligned}$$

At the Fermi energy  $\epsilon(p_3) = \mu$ , some straightforward manipulations yield

$$w_{14} \equiv \int \frac{dp'_2}{2\pi} \overline{W}(p_2, P_1 \rightarrow p'_2, -P_1) = \left( \frac{4\pi e^2}{\kappa} \right)^2 N_I \frac{m^2}{\mu^2} \frac{1}{4\pi} \frac{1}{2eB\gamma(-P_1, P_1)} I(\gamma(-P_1, P_1)), \quad (5.8)$$

where

$$\gamma(p_3, p'_3) \equiv \frac{(p'_3 - p_3)^2 + 1/r_s^2}{2eB}, \quad (5.9)$$

and

$$I(\gamma) \equiv \int_0^\infty dx \frac{x}{x + \gamma} e^{-x} = 1 + \gamma e^\gamma \text{Ei}(-\gamma), \quad (5.10)$$

where Ei being the exponential integral. From Eq.(5.5) we find

$$\tau(P_1) = \frac{P_1}{2\mu w_{14}}. \quad (5.11)$$

This equation and Eq.(5.8) yield

$$\frac{1}{\tau} = \frac{8\pi e^4 N_I}{\kappa^2} \frac{m^2}{\mu \sqrt{\mu^2 - m^2}} \frac{1}{4(\mu^2 - m^2) + 1/r_s^2} I \left( \frac{1}{2eB} (4(\mu^2 - m^2) + 1/r_s^2) \right). \quad (5.12)$$

To compare the result by Argyres and Adams for the non-relativistic fermion in the strong magnetic field region [2], let us substitute  $\mu = m + \epsilon_3$ . Here  $\epsilon_3$  means the kinetic energy in the third direction. We can reproduce the non-relativistic form of the relaxation time by expanding it in  $\frac{\epsilon_3}{m}$ :

$$\frac{1}{\tau} = \frac{\pi e^4 N_I}{\kappa^2 (2m)^{1/2}} \epsilon_z^{-3/2} \frac{I \left( \frac{1}{\omega_0} (4\epsilon_z + \epsilon_s) \right)}{1 + (\epsilon_s/4\epsilon_z)} \left[ 1 - \frac{\epsilon_z}{m} + \mathcal{O} \left( \left( \frac{\epsilon_z}{m} \right)^2 \right) \right], \quad (5.13)$$

where  $\omega_0 = \frac{eB}{m}$ , and  $\epsilon_s = \frac{1}{2mr_s^2}$ .

In the strong magnetic field limit  $eB \rightarrow \infty$ ,  $I \left( \frac{1}{2eB} (4(\mu^2 - m^2) + 1/r_s^2) \right) \rightarrow 1$ , then

$$\frac{1}{\tau} \rightarrow \frac{8\pi e^4 N_I}{\kappa^2} \frac{m^2}{\mu \sqrt{\mu^2 - m^2}} \frac{1}{4(\mu^2 - m^2) + 1/r_s^2}. \quad (5.14)$$

Then we get the interpolating formula between the relativistic and the non-relativistic magnetoconductivities in the strong magnetic field limit as shown in Fig.[9]. While  $1/\tau$  grows as

$$\frac{1}{\tau} \propto (\mu^2 - m^2)^{-1/2} \quad (m/\mu \sim 1), \quad (5.15)$$

in the non-relativistic limit, we find

$$\frac{1}{\tau} \propto m^2 \quad (m/\mu \sim 0), \quad (5.16)$$

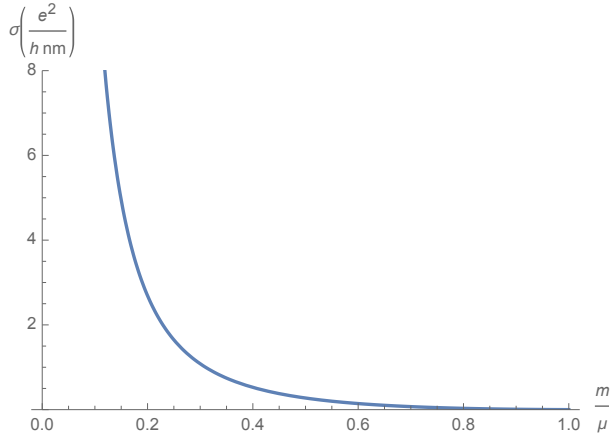


Figure 8: The mass dependence of the magnetoresistance without consideration of inter-cone transition:  $\sigma_{zz}[(e^2/h)/\text{nm}]$  vs.  $m/\mu$ . The parameters:  $\frac{8\pi e^4 N_I}{\kappa^2 \mu^3} \sim 10$ ,  $B \sim 10\text{T}$ ,  $1/r_s^2 \sim \mu \sim 10\text{meV}$ ,  $v_F \sim 10^{15}\text{nm}$ .

in the relativistic limit.

In the massless limit, since  $w_{14}$  goes to zero, the relaxation time goes to infinity, but for the inter-cone transition. It reflects the fact that the helicity does not flip during the impurity scattering in the massless case. However, with the growth of the Fermi energy, terms proportional to a lattice constant  $a$  which are negligible in the low energy effective theory, come into play an effective role in the explicit breaking of the chiral symmetry. Let us consider the terms proportional to the lattice constant in Eq.(2.6), in order to see the region where the effect of the finite lattice constant rather than the mass becomes dominant in chiral symmetry breaking. The mass term in the Hamiltonian is changed into

$$m \rightarrow m + arD^2.$$

The additional term can be written in terms of the canonical momentum

$$\begin{aligned} D^2 &= \pi_1^2 + \pi_2^2 + p_3^2 \\ &= 2eBa^\dagger a + eB + p_3^2. \end{aligned}$$

Therefore the mass term is modified into a momentum-dependent mass

$$M_n(p_3) = m + ar \left[ 2eB \left( n + \frac{1}{2} \right) + p_3^2 \right].$$

Even in massless case, since the effective mass due to the lattice artifact remains non-zero, the intra-cone transition can occur. Then the magnetoconductivity should be suppressed in massless limit like dotted line in Figure 9. If the parameter  $r$  is order 1 and  $eB$  is the same order as the Fermi energy, although  $eB > \mu^2 - m^2$  in the strong magnetic field region, the lattice artifact gives the effective mass in order of  $a\mu^2$ . Therefore when  $m \lesssim a\mu^2$ , the lattice artifact term plays a dominant role in the chiral symmetry breaking. In the typical Dirac semimetals where the negative magnetoresistance is observed, the lattice constant and the Fermi energy are  $a \sim 10\text{eV}^{-1}$ ,  $\mu \sim 0.01\text{eV}$ , respectively [45, 46]. Therefore, in  $m/\mu \lesssim 0.1$  region the lattice artifact is dominant, and if one can open a gap  $m \gtrsim 1\text{meV}$  by breaking the

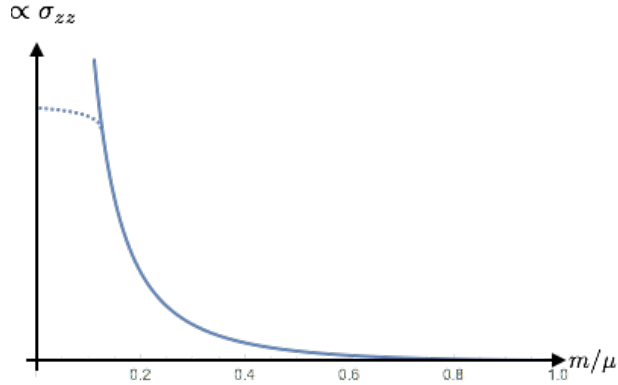


Figure 9: The interpolating function between the relativistic and non-relativistic case for the conductivity:  $\sigma_{zz}$  vs.  $m/\mu$ . The solid line is the estimation without the inter-cone transition. In the massless limit, the effect of the higher derivative terms in the Hamiltonian dominate the relaxation time and suppress the conductivity (dotted line).

crystalline rotational symmetry, the effect can be observed in the experiment. According to Ref.[32], 1% compression will open up a gap of  $\approx 5.6\text{meV}$ , so the effect of the gap by the mechanical strain can be observed.

## 6 Magnetoconductivity in Weaker Magnetic Field

Let us consider what happens as we make the magnetic field weaker. As the magnetic field is weakened, the energy bands of the excited states lower down. After the first excited states touch the Fermi level, these states open as new channels of the scattering. Similar computations of transition amplitude between Landau levels are provided in Ref.[58, 60]. The calculations in those references are treating the case where the chemical potential is below the threshold so that only off-shell transition appears as an intermediate state in the second order perturbation theory. In our calculation the chemical potential is above the threshold so that direct transition from lowest Landau level to higher Landau level is allowed as on-shell transition.

Let us consider the case that only the lowest ( $n = 0, \sigma_3 = +1$ ) and the 1st excited states ( $n = 0, \sigma_3 = -1$ ) and ( $n = 1, \sigma_3 = +1$ ) in Landau levels are below the Fermi energy. Defining  $P_1$  and  $P_2$  as

$$P_1 = \sqrt{\mu^2 - m^2}, \quad (6.1)$$

$$P_2 = \sqrt{\mu^2 - m^2 - 2eB}, \quad (6.2)$$

we find that  $P_*$  in Eq.(4.23) is  $\pm P_1$  for the state with ( $n = 0, \sigma_3 = +1$ ), and  $\pm P_2$  for the states with ( $n = 1, \sigma_3 = +1$ ), ( $n = 0, \sigma_3 = -1$ ), respectively. At zero temperature, only these six set of states (labeled by  $I = 1, \dots, 6$ )[Fig. 10] at the Fermi level contributes to the scattering process. We label these states as

$$1 = (n = 0, \sigma_3 = +1, p_3 = P_1), 2 = (n = 1, \sigma_3 = +1, p_3 = P_2), 3 = (n = 1, \sigma_3 = +1, p_3 = -P_2), \\ 4 = (n = 0, \sigma_3 = +1, p_3 = -P_1), 5 = (n = 0, \sigma_3 = -1, p_3 = P_2), 6 = (n = 0, \sigma_3 = -1, p_3 = -P_2).$$

We denote the corresponding relaxation time  $\tau_I (I = 1, \dots, 6)$  as:

$$\begin{aligned}\tau_1 &= \tau_{0,+}(P_1), \quad \tau_2 = \tau_{1,+}(P_2), \quad \tau_3 = \tau_{1,+}(-P_2), \\ \tau_4 &= \tau_{0,+}(-P_1), \quad \tau_5 = \tau_{0,-}(P_2), \quad \tau_6 = \tau_{0,-}(-P_2).\end{aligned}\quad (6.3)$$

Then from Eq.(4.23), the size of the current can be written as

$$J = \frac{-e^3 B E}{(2\pi)^2 \mu} [P_1(\tau_1 + \tau_4) + P_2(\tau_2 + \tau_3 + \tau_5 + \tau_6)]. \quad (6.4)$$

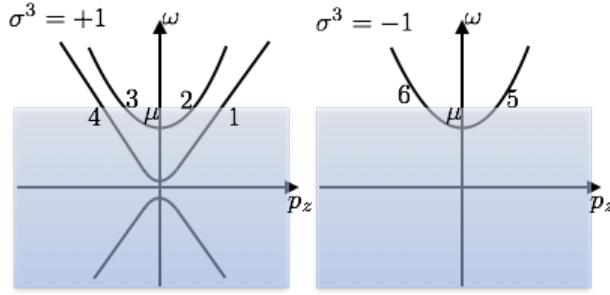


Figure 10: The definition of the labels for the states on the Fermi energy. We keep the same notation even for strong magnetic field case  $2eB > \mu^2 - m^2$ , in which only the states 1 and 4 exist.

From the Fermi's golden rule, the energy is conserved before and after the transition so that the probability can be written as

$$\begin{aligned}W(n, \sigma_3, p_2, p_3 \rightarrow, n', \sigma'_3, p'_2, p'_3) \\ \equiv 2\pi\delta(\epsilon(n, \sigma_3, p_3) - \epsilon(n', \sigma'_3, p'_3))\overline{W}(n, \sigma_3, p_2, p_3 \rightarrow, n', \sigma'_3, p'_2, p'_3).\end{aligned}\quad (6.5)$$

We define  $w_{IJ}$  for  $I, J = 1, \dots, 6$  as

$$w_{IJ} \equiv \int \frac{dp'_2}{2\pi} \overline{W}(I \rightarrow J).$$

From a consideration of symmetries, one expects

$$\begin{aligned}w_{IJ} &= w_{JI}, \quad (I, J = 1, \dots, 6) \\ w_{12} &= w_{43}, \quad w_{13} = w_{42}, \quad w_{15} = w_{46}, \quad w_{16} = w_{54}, \quad w_{25} = w_{63}, \quad w_{26} = w_{53}.\end{aligned}\quad (6.6)$$

Assuming that the impurities are distributed uniformly with density  $N_I$ , we can calculate  $w_{IJ}$  analytically. There are nine independent components of  $w_{IJ}$ :  $w_{12}, w_{13}, w_{14}, w_{15}, w_{16}, w_{23}, w_{25}, w_{26}, w_{56}$ . At the Fermi energy  $\epsilon(n, \sigma_3, p_3) = \mu$ , we can calculate  $w_{IJ}$  in the same way as Sec.5,

$$\begin{aligned}w_{12} &= \left(\frac{4\pi e^2}{\kappa}\right)^2 N_I \frac{[(\mu + m)^2 + P_1 P_2]^2}{4\mu^2(\mu + m)^2} \\ &\quad \times \frac{1}{4\pi} \frac{1}{2eB} \frac{1}{\gamma(P_1, P_2)} [1 - (1 + \gamma(P_1, P_2))I(\gamma(P_1, P_2))],\end{aligned}\quad (6.7)$$

$$w_{13} = \left(\frac{4\pi e^2}{\kappa}\right)^2 N_I \frac{[(\mu + m)^2 - P_1 P_2]^2}{4\mu^2(\mu + m)^2} \times \frac{1}{4\pi} \frac{1}{2eB} \frac{1}{\gamma(P_1, -P_2)} [1 - (1 + \gamma(P_1, -P_2))I(\gamma(P_1, -P_2))], \quad (6.8)$$

$w_{14}$  is given by Eq.(5.8),

$$w_{15} = \left(\frac{4\pi e^2}{\kappa}\right)^2 N_I \frac{4(2eB)P_2^2}{(4\mu)^2(\mu + m)^2} \times \frac{1}{4\pi} \frac{1}{2eB\gamma(P_1, P_2)} [1 - (1 + \gamma(P_1, P_2))I(\gamma(P_1, P_2))], \quad (6.9)$$

$$w_{16} = \left(\frac{4\pi e^2}{\kappa}\right)^2 N_I \frac{4(2eB)P_2^2}{(4\mu)^2(\mu + m)^2} \times \frac{1}{4\pi} \frac{1}{2eB\gamma(P_1, -P_2)} [1 - (1 + \gamma(P_1, -P_2))I(\gamma(P_1, -P_2))], \quad (6.10)$$

$$w_{23} = \left(\frac{4\pi e^2}{\kappa}\right)^2 N_I \frac{4}{(4\mu)^2(\mu + m)^2} \times \frac{2eB}{4\pi} \left[ \left(\frac{2m(\mu + m)}{2eB}\right)^2 \frac{-2 - \gamma(P_2, -P_2) + (3 + 4\gamma(P_2, -P_2) + \gamma^2(P_2, -P_2))I(\gamma(P_2, -P_2))}{\gamma(P_2, -P_2)} + \left(\frac{2m(\mu + m)}{2eB}\right) \frac{-6 - 2\gamma(P_2, -P_2) + (10 + 10\gamma(P_2, -P_2) + 2\gamma^2(P_2, -P_2))I(\gamma(P_2, -P_2))}{\gamma(P_2, -P_2)} + \frac{-4 - \gamma(P_2, -P_2) + (8 + 6\gamma(P_2, -P_2) + \gamma^2(P_2, -P_2))I(\gamma(P_2, -P_2))}{\gamma(P_2, -P_2)} \right], \quad (6.11)$$

$$w_{25} = \left(\frac{4\pi e^2}{\kappa}\right)^2 N_I \frac{8eBP_2^2}{(4\mu)^2(\mu + m)^2} \frac{-1 + (2 + \gamma(P_2, P_2))I(\gamma(P_2, P_2))}{4\pi(2eB)}, \quad (6.12)$$

$$w_{26} = \left(\frac{4\pi e^2}{\kappa}\right)^2 N_I \frac{4P_2^2}{(4\mu)^2(\mu + m)^2} \frac{(\gamma^2(P_2, -P_2) + 4\gamma(P_2, -P_2) + 6)I(\gamma(P_2, -P_2)) - \gamma(P_2, -P_2) - 2}{4\pi\gamma(P_2, -P_2)}, \quad (6.13)$$

$$w_{56} = \left(\frac{4\pi e^2}{\kappa}\right)^2 N_I \frac{4}{(4\mu)^2(\mu + m)^2} \frac{1}{4\pi(2eB)\gamma(P_2, -P_2)} \left[ \{(2eB)^2\gamma^2(P_2, -P_2) + 4eB(6eB + 2m(\mu + m))\gamma(P_2, -P_2) + 4\{m(\mu + m) + 2eB\}\{m(\mu + m) + 4eB\}\} I(\gamma(P_2, -P_2)) - 2eB\{2eB\gamma(P_2, -P_2) + 4(m(\mu + m) + 2eB)\} \right], \quad (6.14)$$

where  $\gamma(p_3, p'_3)$  and  $I(\gamma)$  are defined by Eqs.(5.9), (5.10). Here we used some formulae for  $I(\gamma)$  summarized in Appendix A.

Integrating over  $p'_2, p'_3$ , we obtain from Eq.(4.20)

$$P_I = \sum_{J=1}^6 w_{IJ}(\tau_I P_I - \tau_J P_J) \frac{\mu}{|P_J|}. \quad (6.15)$$

Since the probability distributions  $f$  and  $f_0$  are normalized to unity, their difference satisfies

$$\sum_{n, \sigma_3} \int \frac{d^2 p}{(2\pi)^2} \delta f(n, \sigma_3, p_2, p_3) = 0,$$

from which one obtains using Eq.(4.15)

$$\tau_1 + \tau_2 + \tau_5 - \tau_3 - \tau_4 - \tau_6 = 0. \quad (6.16)$$

Writing down Eq.(6.15) by using the relation for  $w_{ij}$  (6.6), we obtain

$$P_1 = \frac{\mu}{v} \left[ \tau_1 \left\{ (w_{12} + w_{13} + w_{15} + w_{16}) \frac{P_1}{P_2} + w_{14} \right\} - \tau_2 w_{12} + \tau_3 w_{13} + \tau_4 w_{14} - \tau_5 w_{15} + \tau_6 w_{16} \right] \quad (6.17)$$

$$P_2 = \frac{\mu}{v} \left[ -\tau_1 w_{12} + \tau_2 \left\{ (w_{12} + w_{13}) \frac{P_2}{P_1} + w_{23} + w_{25} + w_{26} \right\} + \tau_3 w_{23} + \tau_4 w_{13} - \tau_5 w_{25} + \tau_6 w_{26} \right] \quad (6.18)$$

$$-P_2 = \frac{\mu}{v} \left[ -\tau_1 w_{13} - \tau_2 w_{23} - \tau_3 \left\{ (w_{13} + w_{12}) \frac{P_2}{P_1} + w_{23} + w_{25} + w_{26} \right\} + \tau_4 w_{12} - \tau_5 w_{26} + \tau_6 w_{25} \right] \quad (6.19)$$

$$P_1 = \frac{\mu}{v} \left[ -\tau_1 w_{14} - \tau_2 w_{13} + \tau_3 w_{12} - \tau_4 \left\{ (w_{13} + w_{12} + w_{16} + w_{15}) \frac{P_1}{P_2} + w_{14} \right\} - \tau_5 w_{16} + \tau_6 w_{15} \right] \quad (6.20)$$

$$P_2 = \frac{\mu}{v} \left[ -\tau_1 w_{15} - \tau_2 w_{25} + \tau_3 w_{26} + \tau_4 w_{16} + \tau_5 \left\{ (w_{15} + w_{16}) \frac{P_2}{P_1} + w_{25} + w_{26} + w_{56} \right\} + \tau_6 w_{56} \right] \quad (6.21)$$

$$-P_2 = \frac{\mu}{v} \left[ -\tau_1 w_{16} - \tau_2 w_{26} + \tau_3 w_{25} + \tau_4 w_{15} - \tau_5 w_{56} - \tau_6 \left\{ (w_{16} + w_{15}) \frac{P_2}{P_1} + w_{26} + w_{25} + w_{56} \right\} \right]. \quad (6.22)$$

We solve these simultaneous equations. From (6.17)+(6.20),

$$0 = (w_{12} + w_{13} + w_{15} + w_{16}) \frac{P_1}{P_2} (\tau_1 - \tau_4) - (w_{12} + w_{13})(\tau_2 - \tau_3) - (w_{15} + w_{16})(\tau_5 - \tau_6), \quad (6.23)$$

from (6.18)+(6.19)

$$0 = -(w_{12} + w_{13})(\tau_1 - \tau_4) + \left\{ (w_{12} + w_{13}) \frac{P_2}{P_1} + w_{25} + w_{26} \right\} (\tau_2 - \tau_3) - (w_{25} + w_{26})(\tau_5 - \tau_6), \quad (6.24)$$

and (6.21)+(6.22)

$$0 = -(w_{15} + w_{16})(\tau_1 - \tau_4) - (w_{25} + w_{26})(\tau_2 - \tau_3) + \left\{ (w_{15} + w_{16})\frac{P_2}{P_1} + w_{25} + w_{26} \right\} (\tau_5 - \tau_6). \quad (6.25)$$

Only two equations of these three are independent equations. Combining Eqs.(6.15), the relation of  $w_{IJ}$  (6.6), and the relation between the relaxation times (6.16), we find that the relaxation times on the same bands are equivalent:

$$\tau_1 = \tau_4, \quad \tau_2 = \tau_3, \quad \tau_5 = \tau_6. \quad (6.26)$$

Substituting these into Eqs. (6.17), (6.18), (6.21) and dividing by  $P_1, P_2, P_2$ , respectively we obtain the simultaneous equations

$$1 = \frac{\mu}{v} \left[ \tau_1 \left\{ (w_{12} + w_{13} + w_{15} + w_{16})\frac{1}{P_2} + 2w_{14}\frac{1}{P_1} \right\} - \tau_2(w_{12} - w_{13})\frac{1}{P_1} - \tau_5(w_{15} - w_{16})\frac{1}{P_1} \right] \quad (6.27)$$

$$1 = \frac{\mu}{v} \left[ -\tau_1(w_{12} - w_{13})\frac{1}{P_2} + \tau_2 \left\{ (w_{12} + w_{13})\frac{1}{P_1} + (2w_{23} + w_{25} + w_{26})\frac{1}{P_2} \right\} - \tau_5(w_{25} - w_{26})\frac{1}{P_2} \right] \quad (6.28)$$

$$1 = \frac{\mu}{v} \left[ -\tau_1(w_{15} - w_{16})\frac{1}{P_2} - \tau_2(w_{25} - w_{26})\frac{1}{P_2} + \tau_5 \left\{ (w_{15} + w_{16})\frac{1}{P_1} + (w_{25} + w_{26} + 2w_{56})\frac{1}{P_2} \right\} \right]. \quad (6.29)$$

Solving Eqs.(6.27)-(6.29), we can determine the relaxation times in terms of transfer probabilities. The solution of the these equations are given in Appendix B.

Let us make a remark on the gapless case  $m = 0$ . In Eqs. (6.27), (6.28), (6.29), the quantity  $w_{14}$  vanishes but all other  $w_{ij}$ 's do not vanish and there remains a nontrivial solution for the relaxation time  $\tau_1, \dots, \tau_6$ . This means that for the magnetic field weaker than a critical value  $B_c = \frac{\mu^2}{2e}$  where the higher Landau level contributes to the transition, there is a process where left handed mode is scattered to right-handed mode in the same light-cone mediated by the higher Landau level states even in the massless limit. This effect drastically reduces the conductivity for  $B < B_c$  [Fig.11]. For  $B < B'_c$ , where the second excited states contribute to the transition, further reduction of the conductivity is expected[Fig:12].

This feature is similar to the situation in a carbon nanotube which is a rolled graphene sheet and has two dimensional fermion system. The band structure of the carbon nanotube is known to be

$$\epsilon_{\pm n}(p) = \pm \sqrt{\frac{4\pi^2}{L^2} \left( n - \frac{\nu}{3} \right)^2 + p^2}, \quad n = 0, \pm 1, \pm 2, \dots,$$

where  $L$  is the circumference,  $\nu = 0, \pm 1$  is determined by the helical arrangement [89]. We notice that the band structure has the same form as the Landau levels in Dirac semimetals

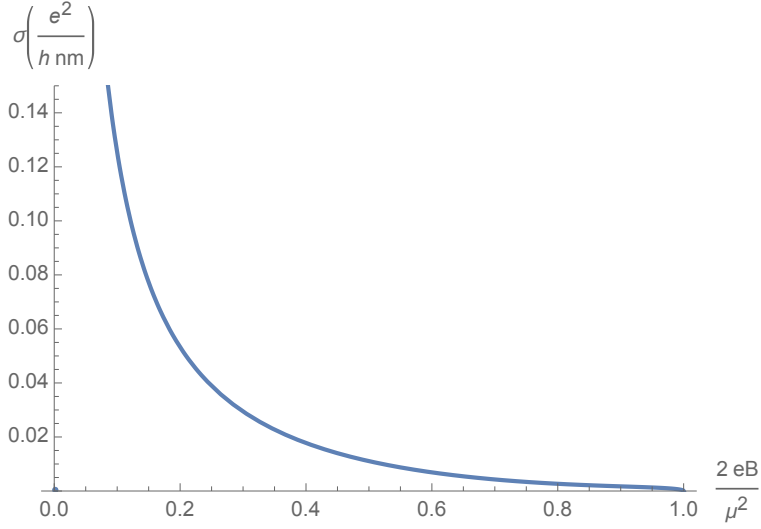


Figure 11: The magnetic field dependence of the conductivity in massless limit:  $\sigma_{zz}[(e^2/h)/\text{nm}]$  vs.  $2eB/\mu^2$ . The parameters:  $\frac{8\pi e^4 N_I}{\kappa^2 \mu^3} \sim 10$ ,  $1/r_s^2 \sim \mu \sim 10\text{meV}$ ,  $v_F \sim 10^{15}\text{nm}$ . We take only the lowest Landau level and the first excited states into account, which is safely applied in the range  $0.5 < 2eB/\mu^2 < 1$ .

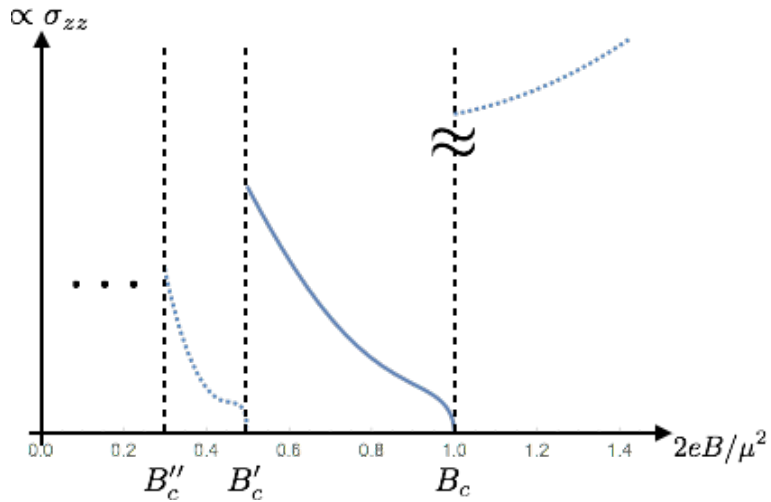


Figure 12: The cartoon figure of the magnetic field dependence of the conductivity:  $\sigma_{zz}$  vs.  $2eB/\mu^2$ . Our result is safely applied in the range  $B'_c < B < B_c$  (solid line). When  $B > B_c$ , since the intra-cone transition is forbidden for massless fermion, only the inter-cone transition contribute to the suppression of the conductivity (dotted line). When  $B < B'_c$ , the second excited states contribute to the intra-cone transition (dotted line).

derived in Subsec.4.1. Besides, it is known that the conductivity changes sensitively as a function of the Fermi energy [90], which comes from the same mechanism as our conductivity as a function of the magnetic field. The different points are following. Our system is originally three dimensional system and so each Landau level has the degeneracy proportional the magnetic field. The interval of each Landau levels can be controlled by changing the magnetic field. As a result, the conductivity in the Dirac semimetals depends both on the magnetic field and the Fermi energy.

## 7 Summary and Discussion

In this thesis, we have studied the relaxation time for the Dirac fermion scattered by the Coulomb impurities, using the action for relativistic Dirac fermion as the low energy effective theory. We have investigated the magnetoconductivity in the Dirac semimetal with mass gap  $m$  from mechanical strain and under magnetic field  $B$  including the regime away from the quantum limit. We have derived the general formula for the relaxation time due to the intra-cone transition, starting from the Boltzmann equation in the relaxation time approximation. Combining with the result of calculation of the transition probability, we have obtained the magnetic dependence of the longitudinal magnetoconductivity.

In the first part, we have seen that the Hamiltonian for the topological insulator and the spin splitting term induced by the magnetic impurity leads to an energy dispersion relation of the Weyl semimetal[74]. Expanding the energy around the Weyl nodes, we have obtained the effective Hamiltonian for the right- and left-handed Weyl fermion with the topology  $\pm 1$ . We have also seen that the stable existence of the Dirac semimetal requires the rotational crystalline symmetry as well as the time reversal and parity symmetry. Therefore it is expected that the gap in the Dirac semimetals opens up when the rotational crystalline symmetry is broken by the mechanical strain[32, 40, 41, 42]. Such massless fermion systems have an analogous effect to the chiral anomaly. In macroscopic system, the chiral anomaly arises as the imbalance between right- and left-handed Fermi energy, and result in the unusual electric current[1].

In the second part, we have investigated the relation between the relaxation time and the current when the multiple Landau levels cross the Fermi energy. The phenomenon of negative magnetoresistance is not only the feature of the Weyl or Dirac semimetals. In fact, although in Ref.[2, 59] they do not assume the existence of the chiral anomaly, they conclude the negative magnetoresistance emerges in the system. The universal existence of the longitudinal magnetotransport for a generic three dimensional metal is also demonstrated in Ref.[91]. We have also derived the general formula for the relaxation time without discussion about the chiral anomaly. On the other hand, even in the same material  $\text{Cd}_3\text{As}_2$ , when its carrier density is very high, the behavior of the observed longitudinal magnetoresistance is not negative, but the usual Shubnikov de Haas oscillation[62]. This experiment indicates that when the lowest Landau level is hidden under the Fermi energy, the negative magnetoresistance due to the chiral anomaly does not emerge. Therefore we have addressed the middle range between the ultra high Fermi energy case and the case in the quantum limit. In this case, each state which crosses the Fermi energy contribute to the scattering, and the relaxation times depend on the momentum of the states. The size of the electric current is given by the sum of the contribution from each states.

Since the realization of the unstable Dirac semimetals requires the very detailed fine tuning of the parameter, the Dirac semimetals used in the experiments[43, 44] have the possibility of the small gap opening. Even in the stable Dirac semimetals, the magnetic field should be applied along a certain direction which preserve the crystalline symmetry which protect the gapless Dirac nodes. Since when the magnetic field direction is deviated from the symmetric direction, the Dirac semimetals used in the experiments[32, 33] may have very small mass gap. Therefore we have computed the effect of mass to the intra-cone transition and obtained the interpolating formula between the relativistic and non-relativistic magnetoconductivity in strong magnetic field region  $2eB > \mu^2 - m^2$ . In massless limit, the relaxation time diverge, because the intra-cone transition does not occur due to the helicity conservation, but for the inter-cone transition. In non-relativistic limit, our result coincide with the previous result calculated by Argyres and Adams [2].

In weak magnetic field region  $2eB < \mu^2 - m^2$ , the property of the relaxation time drastically changes. The first excited states open as new channels of the scattering. Even in massless limit, the intra-cone transition through these states, which does not occur in strong field region, contribute to the finite relaxation times. We have found that as the magnetic field becomes stronger, the conductivity becomes smaller.

At the border of the strong and weaker magnetic field region where the first excited states just touch the Fermi level, one finds  $2eB_c = \mu^2 - m^2$ . In this case Fig.[12] shows that the conductivity goes to zero. This means that at the border of the strong and weak magnetic field the current goes to zero, while the current becomes very large when the magnetic field exceed that point because only the inter-cone transition contribute to the suppression of the conductivity. This phenomenon could be an interesting signal for the longitudinal magnetoconductivity related to the chiral anomaly in the condensed matter system.

In our study, we considered only the lowest and first excited bands. When  $2eB < \frac{\mu^2 - m^2}{2}$ , the second excited states come to contribute to the scattering. So the higher energy band states should be included, when one considers weaker magnetic field case. We considered zero temperature case where scattering by the acoustic phonon can be neglected. However in finite temperature case, we should include the effect of the phonon scattering. Note that the simultaneous equations (6.15) hold when one considers higher excited states or different kind of scattering sources. We focus on the effects on the magnetoconductivity for the Dirac semimetals due to the onset of ‘intra-cone transition’ so that the effects can be described by the low energy effective theory for the single Dirac cone. The inter-cone transition effect should contribute to the relaxation[57, 59, 61], which is highly dependent on the materials and its lattice models.

The electric current induced by the chiral anomaly now getting a renewed interest in the quark gluon plasma[67], the electro-weak plasma in early universe[70], and neutrinos in supernovae[71]. Our approach may also be extended to these systems. Besides, the chiral magnetic effect in the Weyl or Dirac semimetals is an interesting topic not only as the demonstration of the chiral anomaly in the low energy experiment, but also as potential applications in ‘valleytronic’ devices[73].

## Acknowledgments

First of all, I would like to extremely thank my supervisor Tetsuya Onogi for providing great hospitality, substantial discussion, fruitful advice, encouragements throughout all my studies. I also greatly thank Hidenori Fukaya and Satoshi Yamaguchi for carefully reading this thesis and giving meaningful comments. I am deeply grateful to Mikito Koshino for largely enriching knowledge about condensed matter. I also appreciate Shinya Kanemura's various supports and encouragements to complete this thesis. I would also like to thank Koji Hashimoto for taking on the role of the vise-examiner despite sudden offering. I would like further to thank Yukari Nakanishi, Yuji Sugimoto, and all other members of particle physics theory group at Osaka University for encouraging each other and making an excellent learning environment.

## A Formulae for $I(\gamma)$

In this appendix, we summarize the formulae for  $I(\gamma)$  used in Sec.6. The definition of  $I(\gamma)$  is given by

$$I(\gamma) \equiv \int_0^\infty dx \frac{x}{x+\gamma} e^{-x}. \quad (\text{A.1})$$

From

$$\begin{aligned} \int_0^\infty dx \frac{e^{-x}}{x+\gamma} &= \int_0^\infty dx \left( \frac{x+\gamma}{x+\gamma} - \frac{x}{x+\gamma} - \frac{\gamma-1}{x+\gamma} \right) e^{-x} \\ &= 1 - I(\gamma) - (\gamma-1) \int_0^\infty dx \frac{e^{-x}}{x+\gamma}, \end{aligned}$$

we find

$$\gamma \int_0^\infty dx \frac{e^{-x}}{x+\gamma} = 1 - I(\gamma).$$

Therefore we obtain

$$\int_0^\infty dx \frac{e^{-x}}{x+\gamma} = \frac{1 - I(\gamma)}{\gamma}. \quad (\text{A.2})$$

Integration by parts yields

$$\begin{aligned} \int_0^\infty dx \frac{x e^{-x}}{(x+\gamma)^2} &= \int_0^\infty dx \frac{d}{dx} \left( -\frac{1}{x+\gamma} \right) x e^{-x} \\ &= \int_0^\infty dx \frac{1-x}{x+\gamma} e^{-x} \\ &= \frac{1 - I(\gamma)}{\gamma} - I(\gamma) \\ &= \frac{1 - (1+\gamma)I(\gamma)}{\gamma}. \end{aligned} \quad (\text{A.3})$$

Similarly,

$$\begin{aligned} \int_0^\infty dx \frac{e^{-x}}{(x+\gamma)^2} &= \int_0^\infty dx \frac{d}{dx} \left( -\frac{1}{x+\gamma} + \frac{1}{\gamma} \right) e^{-x} \\ &= \int_0^\infty dx \left( -\frac{e^{-x}}{x+\gamma} + \frac{e^{-x}}{\gamma} \right) \\ &= -\frac{1 - I(\gamma)}{\gamma} + \frac{1}{\gamma} \\ &= \frac{I(\gamma)}{\gamma}, \end{aligned} \quad (\text{A.4})$$

and

$$\begin{aligned}
\int_0^\infty dx \frac{x^2 e^{-x}}{(x+\gamma)^2} &= \int_0^\infty dx \frac{(x+\gamma)^2 - 2\gamma x - \gamma^2}{(x+\gamma)^2} e^{-x} \\
&= \int_0^\infty dx \left( 1 - 2\gamma \frac{x}{(x+\gamma)^2} - \gamma^2 \frac{1}{(x+\gamma)^2} \right) e^{-x} \\
&= 1 - 2\gamma \frac{1 - (1+\gamma)I(\gamma)}{\gamma} - \gamma^2 \frac{I(\gamma)}{\gamma} \\
&= -1 + (2+\gamma)I(\gamma).
\end{aligned} \tag{A.5}$$

## B Solution of Equations for Relaxation Times

Simultaneous equations for relaxation times (6.27-6.29) can be written as

$$\begin{pmatrix} 1 \\ 1 \\ 1 \end{pmatrix} = \frac{\mu}{v} \begin{pmatrix} M_{11} & M_{12} & M_{13} \\ M_{21} & M_{22} & M_{23} \\ M_{31} & M_{32} & M_{33} \end{pmatrix} \begin{pmatrix} \tau_1 \\ \tau_2 \\ \tau_5 \end{pmatrix}, \tag{B.1}$$

where

$$M_{11} = (w_{12} + w_{13} + w_{15} + w_{16}) \frac{1}{P_2} + 2w_{14} \frac{1}{P_1}, \tag{B.2}$$

$$M_{12} = -(w_{12} - w_{13}) \frac{1}{P_1}, \tag{B.3}$$

$$M_{13} = -(w_{15} - w_{16}) \frac{1}{P_1}, \tag{B.4}$$

$$M_{21} = -(w_{12} - w_{13}) \frac{1}{P_2}, \tag{B.5}$$

$$M_{22} = (w_{12} + w_{13}) \frac{1}{P_1} + (2w_{23} + w_{25} + w_{26}) \frac{1}{P_2}, \tag{B.6}$$

$$M_{23} = -(w_{25} - w_{26}) \frac{1}{P_2}, \tag{B.7}$$

$$M_{31} = -(w_{15} - w_{16}) \frac{1}{P_2}, \tag{B.8}$$

$$M_{32} = -(w_{25} - w_{26}) \frac{1}{P_2}, \tag{B.9}$$

$$M_{33} = (w_{15} + w_{16}) \frac{1}{P_1} + (w_{25} + w_{26} + 2w_{56}) \frac{1}{P_2}. \tag{B.10}$$

Deriving the inverse matrix of  $M$ , we obtain the relaxation times

$$\tau_1 = \frac{v}{\mu} \frac{M_{13}M_{22} - M_{12}M_{23} - M_{13}M_{32} + M_{23}M_{32} + M_{12}M_{33} - M_{22}M_{33}}{M_{13}M_{22}M_{31} - M_{12}M_{23}M_{31} - M_{13}M_{21}M_{32} + M_{11}M_{23}M_{32} + M_{12}M_{21}M_{33} - M_{11}M_{22}M_{33}} \quad (\text{B.11})$$

$$\tau_2 = \frac{v}{\mu} \frac{-M_{13}M_{21} + M_{11}M_{23} + M_{13}M_{31} - M_{23}M_{31} - M_{11}M_{33} + M_{21}M_{33}}{M_{13}M_{22}M_{31} - M_{12}M_{23}M_{31} - M_{13}M_{21}M_{32} + M_{11}M_{23}M_{32} + M_{12}M_{21}M_{33} - M_{11}M_{22}M_{33}} \quad (\text{B.12})$$

$$\tau_5 = \frac{v}{\mu} \frac{M_{12}M_{21} - M_{11}M_{22} - M_{12}M_{31} + M_{22}M_{31} + M_{11}M_{32} - M_{21}M_{32}}{M_{13}M_{22}M_{31} - M_{12}M_{23}M_{31} - M_{13}M_{21}M_{32} + M_{11}M_{23}M_{32} + M_{12}M_{21}M_{33} - M_{11}M_{22}M_{33}}. \quad (\text{B.13})$$

## References

- [1] H. B. Nielsen and M. Ninomiya, *ADLER-BELL-JACKIW ANOMALY AND WEYL FERMIONS IN CRYSTAL*, *Phys. Lett.* **B130** (1983) 389.
- [2] P. N. Argyres and E. N. Adams, *Longitudinal magnetoresistance in the quantum limit*, *Phys. Rev.* **104** (Nov, 1956) 900–908.
- [3] A. Kagimura and T. Onogi, *Intra-cone transition effect to magnetoconductivity in dirac semimetal*, *Journal of High Energy Physics* **2017** (Dec, 2017) 115.
- [4] S. L. Adler, *Axial-vector vertex in spinor electrodynamics*, *Phys. Rev.* **177** (Jan, 1969) 2426–2438.
- [5] J. S. Bell and R. Jackiw, *A pcac puzzle:  $\pi^0 \rightarrow \gamma\gamma$  in the  $\sigma$ -model*, *Il Nuovo Cimento A (1965-1970)* **60** (Mar, 1969) 47–61.
- [6] D. J. Thouless, M. Kohmoto, M. P. Nightingale and M. den Nijs, *Quantized hall conductance in a two-dimensional periodic potential*, *Phys. Rev. Lett.* **49** (Aug, 1982) 405–408.
- [7] M. Z. Hasan and C. L. Kane, *Colloquium*, *Rev. Mod. Phys.* **82** (Nov, 2010) 3045–3067.
- [8] X.-L. Qi and S.-C. Zhang, *Topological insulators and superconductors*, *Rev. Mod. Phys.* **83** (Oct, 2011) 1057–1110.
- [9] X. Wan, A. M. Turner, A. Vishwanath and S. Y. Savrasov, *Topological semimetal and fermi-arc surface states in the electronic structure of pyrochlore iridates*, *Phys. Rev. B* **83** (May, 2011) 205101.
- [10] A. K. Geim and K. S. Novoselov, *The rise of graphene*, *Nature Materials* **6** (03, 2007) 183.
- [11] A. H. Castro Neto, F. Guinea, N. M. R. Peres, K. S. Novoselov and A. K. Geim, *The electronic properties of graphene*, *Rev. Mod. Phys.* **81** (Jan, 2009) 109–162.

- [12] N. Taira, M. Wakeshima and Y. Hinatsu, *Magnetic properties of iridium pyrochlores  $r_2ir_2o_7$  ( $r = y, sm, eu$  and  $lu$ )*, *Journal of Physics: Condensed Matter* **13** (2001) 5527.
- [13] G. Xu, H. Weng, Z. Wang, X. Dai and Z. Fang, *Chern semimetal and the quantized anomalous hall effect in  $hgcr_2se_4$* , *Phys. Rev. Lett.* **107** (Oct, 2011) 186806.
- [14] H. Zhang, J. Wang, G. Xu, Y. Xu and S.-C. Zhang, *Topological states in ferromagnetic  $cdo/euo$  superlattices and quantum wells*, *Phys. Rev. Lett.* **112** (Mar, 2014) 096804.
- [15] A. A. Burkov and L. Balents, *Weyl semimetal in a topological insulator multilayer*, *Phys. Rev. Lett.* **107** (Sep, 2011) 127205.
- [16] J. Liu and D. Vanderbilt, *Weyl semimetals from noncentrosymmetric topological insulators*, *Phys. Rev. B* **90** (Oct, 2014) 155316.
- [17] S.-M. Huang, S.-Y. Xu, I. Belopolski, C.-C. Lee, G. Chang, B. Wang et al., *A weyl fermion semimetal with surface fermi arcs in the transition metal monophosphide class*, *Nature Communications* **6** (06, 2015) 7373 EP –.
- [18] H. Weng, C. Fang, Z. Fang, B. A. Bernevig and X. Dai, *Weyl semimetal phase in noncentrosymmetric transition-metal monophosphides*, *Phys. Rev. X* **5** (Mar, 2015) 011029.
- [19] S.-Y. Xu, I. Belopolski, N. Alidoust, M. Neupane, G. Bian, C. Zhang et al., *Discovery of a weyl fermion semimetal and topological fermi arcs*, *Science* **349** (2015) 613–617, [<http://science.sciencemag.org/content/349/6248/613.full.pdf>].
- [20] B. Q. Lv, H. M. Weng, B. B. Fu, X. P. Wang, H. Miao, J. Ma et al., *Experimental discovery of weyl semimetal taas*, *Phys. Rev. X* **5** (Jul, 2015) 031013.
- [21] S.-Y. Xu, I. Belopolski, D. S. Sanchez, C. Zhang, G. Chang, C. Guo et al., *Experimental discovery of a topological weyl semimetal state in  $tap$* , *Science Advances* **1** (2015) , [<http://advances.sciencemag.org/content/1/10/e1501092.full.pdf>].
- [22] S.-Y. Xu, N. Alidoust, I. Belopolski, Z. Yuan, G. Bian, T.-R. Chang et al., *Discovery of a weyl fermion state with fermi arcs in niobium arsenide*, *Nature Physics* **11** (08, 2015) 748 EP –.
- [23] I. Belopolski, S.-Y. Xu, Y. Ishida, X. Pan, P. Yu, D. S. Sanchez et al., *Unoccupied electronic structure and signatures of topological Fermi arcs in the Weyl semimetal candidate  $Mo_xW_{1-x}Te_2$* , *ArXiv e-prints* (Dec., 2015) , [[1512.09099](https://arxiv.org/abs/1512.09099)].
- [24] I. Belopolski, S.-Y. Xu, D. S. Sanchez, G. Chang, C. Guo, M. Neupane et al., *Criteria for directly detecting topological fermi arcs in weyl semimetals*, *Phys. Rev. Lett.* **116** (Feb, 2016) 066802.
- [25] S. Murakami, S. Iso, Y. Avishai, M. Onoda and N. Nagaosa, *Tuning phase transition between quantum spin hall and ordinary insulating phases*, *Phys. Rev. B* **76** (Nov, 2007) 205304.

- [26] S. Murakami and S.-i. Kuga, *Universal phase diagrams for the quantum spin hall systems*, *Phys. Rev. B* **78** (Oct, 2008) 165313.
- [27] S. Murakami, *Phase transition between the quantum spin hall and insulator phases in 3d: emergence of a topological gapless phase*, *New Journal of Physics* **9** (2007) 356.
- [28] S.-Y. Xu, Y. Xia, L. A. Wray, S. Jia, F. Meier, J. H. Dil et al., *Topological phase transition and texture inversion in a tunable topological insulator*, *Science* **332** (2011) 560–564, [<http://science.sciencemag.org/content/332/6029/560.full.pdf>].
- [29] T. Sato, K. Segawa, K. Kosaka, S. Souma, K. Nakayama, K. Eto et al., *Unexpected mass acquisition of dirac fermions at the quantum phase transition of a topological insulator*, *Nature Physics* **7** (08, 2011) 840.
- [30] S. M. Young, S. Zaheer, J. C. Y. Teo, C. L. Kane, E. J. Mele and A. M. Rappe, *Dirac semimetal in three dimensions*, *Phys. Rev. Lett.* **108** (Apr, 2012) 140405.
- [31] J. A. Steinberg, S. M. Young, S. Zaheer, C. L. Kane, E. J. Mele and A. M. Rappe, *Bulk dirac points in distorted spinels*, *Phys. Rev. Lett.* **112** (Jan, 2014) 036403.
- [32] Z. Wang, Y. Sun, X.-Q. Chen, C. Franchini, G. Xu, H. Weng et al., *Dirac semimetal and topological phase transitions in  $A_3bi$  ( $a = Na, k, rb$ )*, *Phys. Rev. B* **85** (May, 2012) 195320.
- [33] Z. Wang, H. Weng, Q. Wu, X. Dai and Z. Fang, *Three-dimensional dirac semimetal and quantum transport in  $cd_3as_2$* , *Phys. Rev. B* **88** (Sep, 2013) 125427.
- [34] Z. K. Liu, B. Zhou, Y. Zhang, Z. J. Wang, H. M. Weng, D. Prabhakaran et al., *Discovery of a three-dimensional topological dirac semimetal,  $na_3bi$* , *Science* **343** (2014) 864–867, [<http://science.sciencemag.org/content/343/6173/864.full.pdf>].
- [35] S.-Y. Xu, C. Liu, S. K. Kushwaha, R. Sankar, J. W. Krizan, I. Belopolski et al., *Observation of fermi arc surface states in a topological metal*, *Science* **347** (2015) 294–298, [<http://science.sciencemag.org/content/347/6219/294.full.pdf>].
- [36] M. Neupane, S.-Y. Xu, R. Sankar, N. Alidoust, G. Bian, C. Liu et al., *Observation of a three-dimensional topological Dirac semimetal phase in high-mobility  $Cd_3As_2$* , *Nature Communications* **5** (May, 2014) 3786, [[1309.7892](https://doi.org/10.1038/ncomms7892)].
- [37] Z. K. Liu, J. Jiang, B. Zhou, Z. J. Wang, Y. Zhang, H. M. Weng et al., *A stable three-dimensional topological dirac semimetal  $cd_3as_2$* , *Nat Mater* **13** (07, 2014) 677–681.
- [38] H. Yi, Z. Wang, C. Chen, Y. Shi, Y. Feng, A. Liang et al., *Evidence of topological surface state in three-dimensional dirac semimetal  $cd_3as_2$* , *Scientific Reports* **4** (08, 2014) 6106 EP –.
- [39] S. Borisenko, Q. Gibson, D. Evtushinsky, V. Zabolotnyy, B. Büchner and R. J. Cava, *Experimental realization of a three-dimensional dirac semimetal*, *Phys. Rev. Lett.* **113** (Jul, 2014) 027603.

- [40] S. Jeon, B. B. Zhou, A. Gyenis, B. E. Feldman, I. Kimchi, A. C. Potter et al., *Landau quantization and quasiparticle interference in the three-dimensional dirac semimetal  $cd_3as_2$* , *Nature Materials* **13** (06, 2014) 851.
- [41] I. Zeljkovic, Y. Okada, M. Serbyn, R. Sankar, D. Walkup, W. Zhou et al., *Dirac mass generation from crystal symmetry breaking on the surfaces of topological crystalline insulators*, *Nature Materials* **14** (02, 2015) 318 EP –.
- [42] X. Yuan, P. Cheng, L. Zhang, C. Zhang, J. Wang, Y. Liu et al., *Direct observation of landau level resonance and mass generation in dirac semimetal  $cd_3as_2$  thin films*, *Nano Letters* **17** (2017) 2211–2219, [<http://dx.doi.org/10.1021/acs.nanolett.6b04778>].
- [43] H.-J. Kim, K.-S. Kim, J.-F. Wang, M. Sasaki, N. Satoh, A. Ohnishi et al., *Dirac versus weyl fermions in topological insulators: Adler-bell-jackiw anomaly in transport phenomena*, *Phys. Rev. Lett.* **111** (Dec, 2013) 246603.
- [44] Q. Li, D. E. Kharzeev, C. Zhang, Y. Huang, I. Pletikosic, A. V. Fedorov et al., *Observation of the chiral magnetic effect in  $ZrTe_5$* , *Nature Phys.* **12** (2016) 550–554, [[1412.6543](https://doi.org/10.1038/nphys1412)].
- [45] J. Xiong, S. K. Kushwaha, T. Liang, J. W. Krizan, M. Hirschberger, W. Wang et al., *Evidence for the chiral anomaly in the dirac semimetal  $na_3bi$* , *Science* **350** (2015) 413–416, [<http://science.sciencemag.org/content/350/6259/413.full.pdf>].
- [46] C.-Z. Li, L.-X. Wang, H. Liu, J. Wang, Z.-M. Liao and D.-P. Yu, *Giant negative magnetoresistance induced by the chiral anomaly in individual  $cd_3as_2$  nanowires*, *Nature Communications* **6** (12, 2015) 10137.
- [47] C.-L. Zhang, S.-Y. Xu, I. Belopolski, Z. Yuan, Z. Lin, B. Tong et al., *Signatures of the adler–bell–jackiw chiral anomaly in a weyl fermion semimetal*, *Nature Communications* **7** (02, 2016) 10735.
- [48] X. Huang, L. Zhao, Y. Long, P. Wang, D. Chen, Z. Yang et al., *Observation of the chiral-anomaly-induced negative magnetoresistance in 3d weyl semimetal  $taas$* , *Phys. Rev. X* **5** (Aug, 2015) 031023.
- [49] J. Du, H. Wang, Q. Chen, Q. Mao, R. Khan, B. Xu et al., *Large unsaturated positive and negative magnetoresistance in Weyl semimetal  $TaP$* , *Science China Physics, Mechanics, and Astronomy* **59** (May, 2016) 5798, [[1507.05246](https://doi.org/10.1007/s11464-016-0524-6)].
- [50] Y. Li, Z. Wang, P. Li, X. Yang, Z. Shen, F. Sheng et al., *Negative magnetoresistance in weyl semimetals  $nba_3$  and  $nbp$ : Intrinsic chiral anomaly and extrinsic effects*, *Frontiers of Physics* **12** (Jun, 2017) 127205.
- [51] X. Yang, Y. Liu, Z. Wang, Y. Zheng and Z.-a. Xu, *Chiral anomaly induced negative magnetoresistance in topological Weyl semimetal  $NbAs$* , *ArXiv e-prints* (June, 2015) , [[1506.03190](https://arxiv.org/abs/1506.03190)].
- [52] Y. Wang, E. Liu, H. Liu, Y. Pan, L. Zhang, J. Zeng et al., *Gate-tunable negative longitudinal magnetoresistance in the predicted type-ii weyl semimetal  $wte_2$* , *Nature Communications* **7** (10, 2016) 13142 EP –.

- [53] E. Zhang, R. Chen, C. Huang, J. Yu, K. Zhang, W. Wang et al., *Tunable positive to negative magnetoresistance in atomically thin  $\text{WTe}_2$* , *Nano Letters* **17** (2017) 878–885, [<http://dx.doi.org/10.1021/acs.nanolett.6b04194>].
- [54] T. Ando, T. Nakanishi and R. Saito, *Berry's phase and absence of back scattering in carbon nanotubes*, *Journal of the Physical Society of Japan* **67** (1998) 2857–2862, [<https://doi.org/10.1143/JPSJ.67.2857>].
- [55] X. Dai, H.-Z. Lu, S.-Q. Shen and H. Yao, *Detecting monopole charge in weyl semimetals via quantum interference transport*, *Phys. Rev. B* **93** (Apr, 2016) 161110.
- [56] H.-Z. Lu and S.-Q. Shen, *Weak antilocalization and localization in disordered and interacting weyl semimetals*, *Phys. Rev. B* **92** (Jul, 2015) 035203.
- [57] Y. Ominato and M. Koshino, *Magnetotransport in weyl semimetals in the quantum limit: Role of topological surface states*, *Phys. Rev. B* **93** (Jun, 2016) 245304.
- [58] S.-B. Zhang, H.-Z. Lu and S.-Q. Shen, *Linear magnetoconductivity in an intrinsic topological weyl semimetal*, *New Journal of Physics* **18** (2016) 053039.
- [59] X. Li, B. Roy and S. Das Sarma, *Weyl fermions with arbitrary monopoles in magnetic fields: Landau levels, longitudinal magnetotransport, and density-wave ordering*, *Phys. Rev. B* **94** (Nov, 2016) 195144.
- [60] J. Behrends and J. H. Bardarson, *Strongly angle-dependent magnetoresistance in weyl semimetals with long-range disorder*, *Phys. Rev. B* **96** (Aug, 2017) 060201.
- [61] D. L. Boyda, V. V. Braguta, M. I. Katsnelson and A. Yu. Kotov, *Lattice Quantum Monte Carlo Study of Chiral Magnetic Effect in Dirac Semimetals*, [1707.09810](https://arxiv.org/abs/1707.09810).
- [62] T. Liang, Q. Gibson, M. N. Ali, M. Liu, R. J. Cava and N. P. Ong, *Ultrahigh mobility and giant magnetoresistance in the dirac semimetal  $\text{Cd}_3\text{As}_2$* , *Nature Materials* **14** (11, 2014) 280.
- [63] S. M. Young, S. Chowdhury, E. J. Walter, E. J. Mele, C. L. Kane and A. M. Rappe, *Theoretical investigation of the evolution of the topological phase of  $\text{Bi}_2\text{Se}_3$  under mechanical strain*, *Phys. Rev. B* **84** (Aug, 2011) 085106.
- [64] P. Hosur and X. Qi, *Recent developments in transport phenomena in weyl semimetals*, *Comptes Rendus Physique* **14** (2013) 857 – 870.
- [65] D. T. Son and B. Z. Spivak, *Chiral anomaly and classical negative magnetoresistance of weyl metals*, *Phys. Rev. B* **88** (Sep, 2013) 104412.
- [66] E. V. Gorbar, V. A. Miransky and I. A. Shovkovy, *Chiral anomaly, dimensional reduction, and magnetoresistivity of weyl and dirac semimetals*, *Phys. Rev. B* **89** (Feb, 2014) 085126.
- [67] K. Fukushima, D. E. Kharzeev and H. J. Warringa, *The Chiral Magnetic Effect*, *Phys. Rev. D* **78** (2008) 074033, [[0808.3382](https://arxiv.org/abs/0808.3382)].

- [68] C. Manuel and J. M. Torres-Rincon, *Dynamical evolution of the chiral magnetic effect: Applications to the quark-gluon plasma*, *Phys. Rev. D* **92** (Oct, 2015) 074018.
- [69] M. Ruggieri, G. X. Peng and M. Chernodub, *Chiral relaxation time at the crossover of quantum chromodynamics*, *Phys. Rev. D* **94** (Sep, 2016) 054011.
- [70] M. Joyce and M. E. Shaposhnikov, *Primordial magnetic fields, right-handed electrons, and the Abelian anomaly*, *Phys. Rev. Lett.* **79** (1997) 1193–1196, [[astro-ph/9703005](#)].
- [71] N. Yamamoto, *Chiral transport of neutrinos in supernovae: Neutrino-induced fluid helicity and helical plasma instability*, *Phys. Rev.* **D93** (2016) 065017, [[1511.00933](#)].
- [72] T. Osada, *Negative interlayer magnetoresistance and zero-mode Landau level in multilayer Dirac electron systems*, *Journal of the Physical Society of Japan* **77** (2008) 084711, [<https://doi.org/10.1143/JPSJ.77.084711>].
- [73] S. A. Parameswaran, T. Grover, D. A. Abanin, D. A. Pesin and A. Vishwanath, *Probing the chiral anomaly with nonlocal transport in three-dimensional topological semimetals*, *Phys. Rev. X* **4** (Sep, 2014) 031035.
- [74] D. Kurebayashi and K. Nomura, *Weyl semimetal phase in solid-solution narrow-gap semiconductors*, *Journal of the Physical Society of Japan* **83** (2014) 063709, [<https://doi.org/10.7566/JPSJ.83.063709>].
- [75] B.-J. Yang and N. Nagaosa, *Classification of stable three-dimensional Dirac semimetals with nontrivial topology*, *Nature Communications* **5** (Sept., 2014) 4898, [[1404.0754](#)].
- [76] C. Fang, M. J. Gilbert, X. Dai and B. A. Bernevig, *Multi-Weyl topological semimetals stabilized by point group symmetry*, *Phys. Rev. Lett.* **108** (Jun, 2012) 266802.
- [77] S.-Y. Xu, C. Liu, S. K. Kushwaha, T.-R. Chang, J. W. Krizan, R. Sankar et al., *Observation of a bulk 3D Dirac multiplet, Lifshitz transition, and nested spin states in Na<sub>3</sub>Bi*, *ArXiv e-prints* (Dec., 2013) , [[1312.7624](#)].
- [78] K. Fujikawa and H. Suzuki, *Path integrals and quantum anomalies*. 2004. 10.1093/acprof:oso/9780198529132.001.0001.
- [79] V. Aji, *Adler-Bell-Jackiw anomaly in Weyl semimetals: Application to pyrochlore iridates*, *Phys. Rev. B* **85** (Jun, 2012) 241101.
- [80] A. A. Zyuzin and A. A. Burkov, *Topological response in Weyl semimetals and the chiral anomaly*, *Phys. Rev. B* **86** (Sep, 2012) 115133.
- [81] M. M. Vazifeh and M. Franz, *Electromagnetic response of Weyl semimetals*, *Phys. Rev. Lett.* **111** (Jul, 2013) 027201.
- [82] D. A. Pesin, E. G. Mishchenko and A. Levchenko, *Density of states and magnetotransport in Weyl semimetals with long-range disorder*, *Phys. Rev. B* **92** (Nov, 2015) 174202.

- [83] C.-Z. Chen, H. Liu, H. Jiang and X. C. Xie, *Positive magnetoconductivity of weyl semimetals in the ultraquantum limit*, *Phys. Rev. B* **93** (Apr, 2016) 165420.
- [84] A. Jimenez-Alba, K. Landsteiner, Y. Liu and Y.-W. Sun, *Anomalous magnetoconductivity and relaxation times in holography*, *Journal of High Energy Physics* **2015** (Jul, 2015) 117.
- [85] E.-d. Guo and S. Lin, *Quark mass effect on axial charge dynamics*, *Phys. Rev. D* **93** (May, 2016) 105001.
- [86] Y.-W. Sun and Q. Yang, *Negative magnetoresistivity in holography*, *Journal of High Energy Physics* **2016** (Sep, 2016) 122.
- [87] A. Kagimura and T. Onogi, *Relaxation time of the fermions in the magnetic field (I) - the case for relativistic fermions -*, *PoS LATTICE2016* (2016) 379.
- [88] T. Onogi and A. Kagimura, *Relaxation time of the fermions in the magnetic field (II) - away from strong magnetic field limit -*, *PoS LATTICE2016* (2016) 381.
- [89] H. Ajiki and T. Ando, *Electronic states of carbon nanotubes*, *Journal of the Physical Society of Japan* **62** (1993) 1255–1266.
- [90] T. Serii and T. Ando, *Boltzmann conductivity of a carbon nanotube in magnetic fields*, *Journal of the Physical Society of Japan* **66** (1997) 169–173.
- [91] P. Goswami, J. H. Pixley and S. Das Sarma, *Axial anomaly and longitudinal magnetoresistance of a generic three-dimensional metal*, *Phys. Rev. B* **92** (Aug, 2015) 075205.